Published in final edited form as:

Cell Rep. 2024 April 23; 43(4): 113998. doi:10.1016/j.celrep.2024.113998.

Initiation of a ZAKα-dependent ribotoxic stress response by the innate immunity endoribonuclease RNase L

Jiajia Xi[1,*], **Goda Snieckute**[2,3], **José Francisco Martínez**[2,3], **Frederic Schrøder Wenzel Arendrup**[4], **Abhishek Asthana**[1], **Christina Gaughan**[1], **Anders H. Lund**[4], **Simon Bekker-Jensen**[2,3,*], **Robert H. Silverman**[1,5,*]

[1]Department Cancer Biology, Cleveland Clinic Foundation, Lerner Research Institute, Cleveland, OH 44195, USA

[2]Center for Healthy Aging, Department of Cellular and Molecular Medicine, University of Copenhagen, Blegdamsvej 3B, 2200 Copenhagen, Denmark

[3]Center for Gene Expression, Department of Cellular and Molecular Medicine, University of Copenhagen, Blegdamsvej 3B, 2200 Copenhagen, Denmark

[4]Biotech Research and Innovation Center, University of Copenhagen, Ole Maaløes Vej 5, 2200 Copenhagen, Denmark

[5]Lead contact

SUMMARY

RNase L is an endoribonuclease of higher vertebrates that functions in antiviral innate immunity. Interferons induce oligoadenylate synthetase enzymes that sense double-stranded RNA of viral origin leading to the synthesis of 2′,5′-oligoadenylate (2-5A) activators of RNase L. However, it is unknown precisely how RNase L remodels the host cell transcriptome. To isolate effects of RNase L from other effects of double-stranded RNA or virus, 2-5A is directly introduced into cells. Here, we report that RNase L activation by 2-5A causes a ribotoxic stress response involving the MAP kinase kinase kinase (MAP3K) ZAKα, MAP2Ks, and the stress-activated protein kinases JNK and p38α. RNase L activation profoundly alters the transcriptome by widespread depletion of mRNAs associated with different cellular functions but also by JNK/p38α-stimulated induction of inflammatory genes. These results show that the 2-5A/RNase L system triggers a protein kinase cascade leading to proinflammatory signaling and apoptosis.

In brief

*Correspondence: xij@ccf.org (J.X.), sbj@sund.ku.dk (S.B.-J.), silverr@ccf.org (R.H.S.).

AUTHOR CONTRIBUTIONS

Conceptualization, J.X., S.B.-J., and R.H.S.; investigation, J.X., G.S., J.F.M., F.S.W.A., A.A., C.G., and A.H.L.; writing – original draft, J.X. and R.H.S.; writing – review & editing, J.X., S.B.-J., and R.H.S.; funding acquisition, R.H.S. and S.B.-J.; supervision, R.H.S. and S.B.-J.

DECLARATION OF INTERESTS

The authors declare no competing interests.

SUPPLEMENTAL INFORMATION

Supplemental information can be found online at https://doi.org/10.1016/j.celrep.2024.113998.

In response to viral double-stranded RNA, OAS enzymes produce 2′,5′-oligoadenylates, known as 2-5As, which activate RNase L. J. Xi et al. show that RNase L activity triggers ZAKα to phosphorylate MAP2Ks that signal to JNK and p38α, leading to inflammatory signaling and apoptosis.

Graphical Abstract.

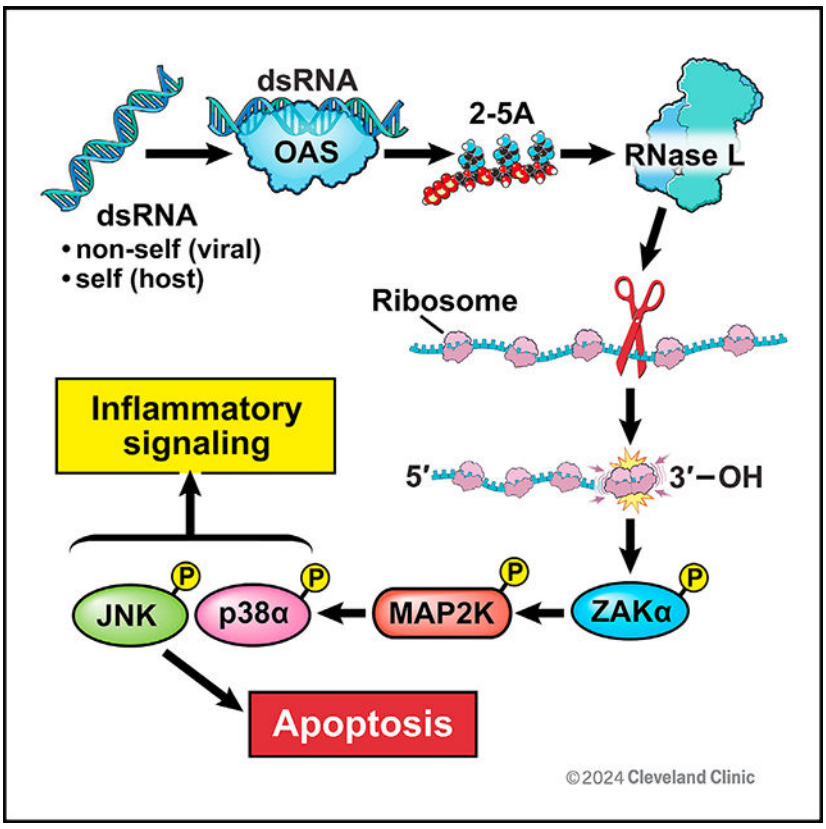

INTRODUCTION

A wide range of different cellular insults trigger stress responses that determine cell survival and cell fate.[1] Adaptation and survival of the injured cell is accompanied by inflammatory signaling. However, the cell dies when the damage exceeds the capacity of the cell to repair. A ribotoxic stress response is a type of cellular stress pathway in which RNA damage or translational insults cause ribosomes to stall and/or collide.[1–4] Ribotoxic stressors include ribotoxins that cleave 28S rRNA (Shiga toxin, α-sarcin, and ricin); some, but not all, antibiotics that inhibit translational elongation (anisomycin, cycloheximide); and ultraviolet radiation that damages mRNA.[1,4,5] Ribotoxic stress is sensed by the MAP kinase kinase kinase (MAP3K) ZAKα, a mixed-lineage kinase that interacts with actively translating ribosomes. Following activation, ZAKα phosphorylates the MAP2Ks 3/6 and 4/7.[6] Subsequently, the MAP2Ks phosphorylate the stress-activated MAPKs (SAPKs) JNK and p38α. There are two ZAK isoforms: a longer form, ZAKα, with a flexible C-terminal segment that contains two regions and which binds to ribosomes, and a short

form, ZAKβ, that neither associates with ribosomes nor is involved in the ribotoxic stress response.[3] ZAKα phosphorylation in response to ribotoxic stress leads to its dissociation from ribosomes and phosphorylation of SAPKs.[3] Activation of JNK and p38α stimulates proinflammatory signaling, while activation of JNK also leads to apoptosis.[7]

RNase L is a regulated endoribonuclease that functions in antiviral innate immunity downstream of the interferon (IFN)-induced 2′,5′-oligoadenylate synthetases (OASs).[8,9] Double-stranded RNA (dsRNA), of either viral or cellular origin, activates IFN-inducible OASs 1–3.[10,11] Once activated by dsRNA, these OASs produce 5′-phosphorylated 2′,5′-oligoadenylates (known as 2-5As) from ATP.[9,12,13] 2-5A binding to RNase L in the presence of ATP causes its dimerization and activation.[14–16] RNase L is a general endoribonuclease that cleaves single-strand RNAs (ssRNAs) predominantly at UpUp^N and UpAp^N sites, restricting protein synthesis through endonucleolytic cleavage of actively translating mRNAs.[17–21] The antiviral activity of RNase L is accompanied by degradation of viral and cellular ssRNAs.[22] Moreover, RNase L also cleaves rRNA in intact ribosomes, as well as some tRNAs.[19,23,24] Interestingly, RNase L activation following transfection with 2-5A or dsRNA leads to phosphorylation of JNK.[25,26] In addition, JNK activation by RNase L beyond a poorly defined threshold leads to apoptosis.[25,27] Here, we show that 2-5A activation of RNase L leads to imbalanced transcriptome changes and a ZAKα-dependent ribotoxic stress response involving proinflammatory signaling and apoptosis.

RESULTS

ZAKα is required for the 2-5A/RNase L-induced ribotoxic stress response

To study the impact of RNase L on the ribotoxic stress response and innate immune gene expression, primary macrophages were initially used because they have high levels of RNase L and are a source of proinflammatory cytokines and chemokines during virus infections.[28,29] To specifically activate RNase L, 2-5A ($p_3$5′A2′p5′A2′p5′A) was transfected into wild-type (WT) mouse bone marrow macrophages (BMMs) (Figures S1 and S2A). 2-5A stimulated RNase L in a dose- and time-dependent manner (≥2 μM; ≥2 h) as determined by the appearance of characteristic, discrete rRNA cleavage products (Figures 1A and 1B).[23,24] Breakdown of 28S and 18S rRNA was observed in WT BMMs transfected with 2-5A but not with dephosphorylated 2-5A (A3), included as a negative control, whereas neither 2-5A nor A3 induced rRNA cleavage in RNase L knockout (KO) BMMs (Figure 1C). Therefore, rRNA cleavage induced by 2-5A was due to RNase L activity and only in response to authentic 2-5A. In addition, prolonged incubation with 2-5A (>5 h) led to the death of WT BMMs but not of RNase L KO BMMs (Figure 1D).

Previously, we reported that RNase L activation induced JNK phosphorylation in response to dsRNA, 2-5A, or virus infection.[25,26] To probe the molecular mechanism of the 2-5A/RNase L-induced ribotoxic stress response, phosphorylation of JNK, p38α, and ERK1/2 was monitored during 2-5A transfections. In WT BMMs, but not in RNase L KO BMMs, 2-5A induced phosphorylation of JNK beginning at 30–45 min (Figure 1E). There were also low basal levels of p38α phosphorylation in the WT BMMs, which were increased following 2-5A transfection within a similar time frame. However, ERK1/2 was not phosphorylated

in response to 2-5A transfection of WT BMMs, suggesting that the 2-5A/RNase L-induced ribotoxic stress caused JNK and p38α, but not ERK, signaling.

Because the ribosome-associated MAP3K ZAKα phosphorylates MAP2Ks that then phosphorylate the MAPKs JNK and p38α and is a sensor for many different ribotoxic stressors,[1] the possibility that it might be activated by 2-5A-induced RNase L activity was investigated. Remarkably, phosphorylation of JNK and p38α in response to 2-5A and RNase L was abrogated in ZAK KO BMMs (Figure 1F). There was, however, no effect of ZAKα on the ribonuclease activity of RNase L (Figure 1F, bottom). Furthermore, a small-molecule ZAK inhibitor (ZAKi; compound 3h), which blocks the kinase activity of ZAKα,[30] greatly reduced 2-5A-induced phosphorylation of MAP2K3/MAP2K6, MAP2K4, JNK, and p38α without affecting the ribonuclease activity of RNase L (Figure 1G). These data show that ZAKα is required for 2-5A/RNase L-induced MAP2K, JNK, and p38α phosphorylation in a kinase-dependent manner during the ribotoxic stress response.

2-5A activation of RNase L modulates the macrophage transcriptome by degrading and inducing different transcripts

To probe 2-5A-induced global effects on the transcriptome, WT BMMs and RNase L KO BMMs were either mock transfected or transfected with 2-5A or A3 followed by bulk RNA sequencing (RNA-seq) (Figure S2A). Transcriptomes of the 2-5A-transfected WT BMMs were significantly different from all other treatment groups, indicating that RNase L activity dramatically altered transcript expression (Figure 2A). The differentially expressed genes (DEGs) for every condition were compared and cross-analyzed (Figure 2B, S2B–S2E). There were 4,843 DEGs in 2-5A-stimulated WT BMMs, comprising about 20% of the total transcripts sequenced (Figure 2B; Table S2). In contrast, there were no DEGs in A3-transfected WT BMMs nor in 2-5A- or A3-transfected RNase L KO BMMs. Among these DEGs were 3,334 genes with reduced expression (presumably due to RNA degradation) and 1,509 genes with increased expression (Figure 2C). Given that RNase L is a general ribonuclease with only modest specificity, the observation that a minority of transcripts were decreased in abundance suggested that some transcripts might be preferentially degraded by RNase L.[18] These results are in contrast to studies showing 70%–90% mRNA degradation in dsRNA poly(I):poly(C) (pIC)-transfected cells.[20,21] The differences in the extent of RNA degradation are likely due to differences in the level and duration of RNase L activation between the two types of protocols, i.e., 2-5A transfection or pIC transfection, and to differences in expression levels of RNase L in the different cell types.

To better understand the functional impact of 2-5A-induced RNase L activity on the transcriptome, gene set enrichment analysis (GSEA) was performed based on the DEG ranking from 2-5A-transfected WT BMM RNA-seq. Among hallmark gene sets, which classify genes according to their participation in biological states or processes, there were predominantly decreases (negative enrichment) of transcripts related to gene sets corresponding to IFNα and IFNγ responses, protein secretion, and mTORC1 signaling (Figure 2D). In contrast, there was a relative increase (positive enrichment) of transcripts in the “tumor necrosis factor α (TNF-α) signaling via nuclear factor κB (NF-κB)” gene set, including many genes encoding proinflammatory proteins (e.g., interleukin [IL]-6, TNF)

and transcription factors (e.g., Jun, Fosb) (Figures 2D and 2E). In addition, GSEA Gene Ontology (GO) analysis based on functions of genes and gene products indicated that RNase L predominantly reduced levels of certain transcript groups, including for antigen processing and presentation, small ribosomal subunit, IFNα production, regulation of defense to virus, and the innate immune response (Figure S3A). Effects of 2-5A/RNase L on transcripts for small ribosomal subunit proteins could possibly contribute to ribosomal stress. On the other hand, 2-5A stimulation positively enriched acute phase response transcripts, including proinflammatory genes (Figure S3A).

Downregulated transcripts from 2-5A-transfected WT BMMs are represented in heatmaps for IFN-stimulated genes (ISGs) and antiviral genes (Figure S3B), antigen processing and presentation (Figure S3C), ribosomal protein genes (Figure S4A), and housekeeping genes (Figure S4B). Slight upregulation of ISG transcripts in mock- or A3-transfected cells is likely a non-specific response to transfection reagents.[32] In accord with GSEA, the proinflammatory genes downstream of TNF-α, especially those related to stress responses, were induced in WT BMMs upon 2-5A stimulation (Figure 2E). In addition, we confirmed 2-5A induction of the growth differentiation factor 15 gene (GDF15) from a prior study[33] and added it to the heatmap (Figure 2E). These data indicate that 2-5A-stimulated RNase L activity led to bidirectional changes in levels of different transcripts with increases in proinflammatory and stress-responsive transcripts but decreases in many other transcripts, including those involved in IFN responses, antigen processing and presentation, and small ribosome subunit proteins.

2-5A/RNase L induces a proinflammatory transcriptome signature in BMM through *de novo* mRNA synthesis

To validate the GSEA, levels of representative transcripts from different categories of genes were monitored by RT-qPCR. Transcripts that decreased in relative amounts after 2-5A treatment of WT BMMs included those in IFN responses (Ifit1bl1, Stat1, Irf7, Gbp2, Rsad2), inflammation (Cxcl9), and antigen processing and presentation (H2-Aa1, H2-Eb1, Cd86). Transcripts that increased in abundance in 2-5A-transfected WT BMMs included those from TNF-α-regulated genes and stress-response genes (Cxcl2, Gdf15, IL-1β, IL-23α) (Figure 3A). These changes were not observed in 2-5A-transfected RNase L KO BMMs. Results were normalized to GAPDH mRNA levels (Figure 3A). Because RNase L activation decreased mRNA levels for housekeeping genes, including GAPDH mRNA, transcript levels were separately normalized by input mRNA levels (Figures 3B and S4B). Nevertheless, transcript levels displayed similar changes when normalized to levels of input mRNA (Figure 3B). Those results suggested that positive enrichment was due to increases in levels of transcripts related to proinflammatory responses.

To determine if the 2-5A/RNase L-induced transcripts reflected transcriptional induction or resistance to RNase L ribonuclease activity, WT BMMs were treated with actinomycin D to block transcription during 2-5A transfection. Indeed, actinomycin D greatly inhibited the increases in transcript levels suggesting transcriptional induction in response to 2-5A (Figures 3C–3F). Current findings are consistent with the prior observation of transcriptional

induction of the GDF15 gene in response to 2-5A activation of RNase L[33] (Figures 2E and 3E).

2-5A stimulation of RNase L is a downstream effect of dsRNA activation of OAS enzymes. However, dsRNA also stimulates other pathways, notably mitochondrial antiviral signaling protein (MAVS)/IRF3 signaling and protein kinase R (PKR).[34,35] Therefore, regulation of select transcripts were compared in WT and RNase L KO BMMs transfected with either pIC or 2-5A. Results showed that levels of some pIC-inducible transcripts were decreased following 2-5A transfection of WT BMM, likely due to RNase L-mediated mRNA degradation (Figures 4A–4H). On the other hand, some proinflammatory genes induced by 2-5A (CXCL2, IL-1β, and IL-23α) were also induced upon pIC stimulation in WT BMMs (Figures 4I–4K). These results emphasize why it was necessary to use 2-5A to identify transcripts that are specifically regulated by RNase L.

The MAP kinase cascade induces inflammatory gene transcripts in response to 2-5A

To investigate how proinflammatory genes were induced by 2-5A, different pathways were considered. Possible involvement of NF-κB was suggested by analysis of RNA-seq results (Figure 2D). However, 2-5A transfection of A549 cells did not induce NF-κB p65 subunit migration from cytoplasm to nucleus, in contrast to TNF treatment, which did result in localization of NF-κB p65 to nuclei (Figures S5A and S5B, respectively). Also, inhibition of the NF-κB upstream kinase IKK-α did not affect levels of 2-5A-induced transcripts (Figure S5C). In contrast, TNF-α -induced transcripts were suppressed by the IKK-α inhibitor (Figure S5D). Involvement of the MAVS-IRF3 pathway was considered because of cell-type-dependent effects of RNase L on IFN induction.[28,36] However, 2-5A induction of transcripts for Cxcl2, IL-1β, and IL-6 was not prevented by deletion of MAVS in A549 cells (Figure S5E). Finally, the JNK/p38α pathway was considered because of its involvement in ribotoxic stress responses and its activation during TNF-α signaling.[6] JNK and p38α and their downstream transcription factor AP-1 component c-Jun were phosphorylated upon 2-5A stimulation of WT BMMs (Figures 1E and 5A).[37] An inhibitor of p38α (p38αi) prevented 2-5A induction of Cxcl2, Fosb, Gdf15, and IL-23α but not IL-1β (Figure 5B). An inhibitor of JNK (JNKi) reduced 2-5A induction of all transcripts except IL-23α (Figure 5C), whereas AP-1i, an inhibitor of transcription factor AP-1 downstream of JNK/p38α, suppressed induction of all transcripts examined (Figure 5D). These results suggest that p38α and JNK, but not NF-κB or MAVS, were involved in 2-5A induction of transcription for at least some of the proinflammatory genes.

Because ZAKα is an upstream kinase for JNK and p38α phosphorylation, WT BMMs and ZAK KO BMMs were compared for effects of 2-5A on gene induction. Levels of all five transcripts examined were significantly reduced in ZAK KO BMMs compared to the WT BMMs (Figure 5E). Similarly, a ZAKi (compound 3h) reduced 2-5A induction of all five transcripts in WT BMMs (Figure 5F). These results suggest that ZAKα is required for 2-5A induction of these proinflammatory genes in a kinase-activity-dependent manner.

ZAKα is required for the 2-5A/RNase L-induced ribotoxic stress response in human monocytes

To extend these findings to a human immune cell type, ZAK was knocked out in the human monocytic cell line THP-1. The human homologs of some representative genes from the BMM studies were examined in the THP-1 cells with similar observed changes upon 2-5A transfection when normalized to SON-DNA- and-RNA-binding protein (SON) mRNA, which is resistant to RNase L cleavage (Figures 6A and 6B).[21] Transcripts for Cxcl2, Fosb, Gdf15, IL-1β, and IL-23α were induced by 2-5A transfection of WT THP-1 cells but not in RNase L KO THP-1 cells (Figure 6A).

Furthermore, phosphorylation of both 2-5A- and anisomycin-induced JNK/p38α was impaired in THP1 cells lacking ZAK (Figure 6C). In contrast, while RNase L KO prevented 2-5A-induced phosphorylation of JNK and p38α, the absence of RNase L had no effect on anisomycin-induced activation of JNK and p38α (Figure 6D). Previously, it was determined that intermediate doses of anisomycin inhibit translation and promote ribosome collisions while high doses (up to 100 μg/mL) cause cell death.[4] Therefore, in these studies, an intermediate dose of anisomycin (5 mg/mL) was used. Our results show that 2-5A/RNase L specifically induces ZAKα signaling during the ribotoxic stress response in both human monocytes and mouse bone-marrow-derived macrophages.

RNase L activity contributes to ribosome collisions, ZAKα activation, and apoptosis of cancer cells

Because evasion of apoptosis is a hallmark of cancer,[38] the possible role of ZAKα in apoptosis triggered by 2-5A/RNase L was investigated in A549 cells derived from a human lung adenocarcinoma. To show that ZAKα was phosphorylated in response to 2-5A, gel mobility shift assays were done with Phos-Tag gels (Figure 7A). In this method, the slower-migrating phosphorylated ZAKα is separated from unphosphorylated ZAKα.[4] Either 2-5A or anisomycin caused ZAKα auto-phosphorylation as determined by the mobility shift. Anisomycin was more effective than 2-5A in causing phosphorylation of p38α and JNK (Figure 7A). In addition, two ZAKis (compounds 3h and 6p)[30,39] suppressed phosphorylation of ZAKα and its downstream MAPKs, JNK and p38α, in response to either 2-5A or anisomycin. These results show that ZAKα kinase activity is necessary for 2-5A-induced JNK and p38α activation.

To investigate the involvement of ZAKα and RNase L in apoptosis of A549 cells, these proteins were deleted from A549 cells singly (KO) and in combination (i.e., double KO [DKO]). RNase L KO inhibited both poly(ADP-ribose) polymerase (PARP) cleavage and JNK/p38α phosphorylation upon 2-5A transfection. Similarly, 2-5A-induced JNK/p38α phosphorylation and PARP cleavage were inhibited in ZAK KO and ZAKα/RNase L DKO cells (Figure 7B). Also, 2-5A induction of Gdf15, IL-23α, Cxcl2, Fosb, and IL-1β transcripts was inhibited in RNase KO, ZAK KO, and ZAK/RNase L DKO cells (Figures 7C, 7D, and S6A–S6C).

Cell death in response to 2-5A was monitored by cell staining and real-time imaging of cells. 2-5A transfection of WT A459 cells resulted in a dramatic increase in cell death

(Figures 7E–7G and S6D). In contrast, in both RNase L KO and RNase L/ZAK DKO cells, there was no increase in cell death after 2-5A transfection, despite unexplained low levels of p38α-P and JNK-P in response to 2-5A in RNase L KO A549 cells (Figures 7B, 7E, 7G, and 7H). Deletion of ZAKα alone greatly inhibited cell death (by about 50%) in response to 2-5A, compared to similarly treated WT cells, consistent with the involvement of ZAKα in RNase L-mediated cell death (Figure 7F). However, there remained a small increase in cell death (about 20%) in response to 2-5A in ZAK KO cells, possibly indicating an alternative, non-apoptotic pathway of 2-5A/RNase L-induced cell death, as there was no detectable PARP cleavage (Figures 7B and 7F).

To determine if RNase L activation leads to ribosome collisions, polysomes were digested with micrococcal nuclease followed by separation in sucrose gradients. A modest increase in di- and tri-somes was observed in 2-5A-transfected WT A549 cells but not in identically treated RNase L KO A549 cells (Figure 7I). Results suggest that RNase L activity results in ribosome collisions.

To ascertain if 2-5A activation of RNase L induced protein expression from select genes, western blots were performed. For instance, inhibition of nuclear transport of mRNAs by RNase L could prevent protein expression from induced genes.[40,41] Therefore, protein expression levels of Fosb, Jun, and IL-1β were monitored in western blots after 2-5A transfection of A549 cells. All three proteins were induced, indicating that these proteins, as well as their mRNAs, increased following 2-5A transfection (Figure S7A).

Involvement of ZAKα in dsRNA-induced SAPK phosphorylation and apoptosis

Because dsRNA activates OAS enzymes to produce 2-5A, the impact of ZAK on stress responses during pIC transfection was investigated. Results show that ZAK KO substantially decreased pIC induction of PARP cleavage and phosphorylation of p38α and JNK (Figure S7B). Residual PARP cleavage and p38α and JNK phosphorylation in pIC-transfected ZAK KO cells could be due to alternative MAP3Ks and/or to PKR. However, PKR KO did not inhibit 2-5A-induced phosphorylation of p38α and JNK or PARP cleavage (Figures S7C and S7D). These data support our conclusion that ZAKα is a mediator of proinflammatory and cell death signaling in response to direct activation of RNase L by 2-5A.

DISCUSSION

Impact of RNase L on innate immune signaling

Our results show that RNA degradation by RNase L triggers a kinase cascade that leads to innate immune signaling and apoptosis. These events are set in motion when dsRNA binds and activates OAS enzymes that produce the unusual allosteric effector of RNase L, 2-5A. Innate immune signaling is often initiated by the presence of dsRNA in the cytoplasm. Many RNA and DNA viruses produce non-self-dsRNA as intermediates or by-products of their infection cycles. However, even in the absence of viral infections, cells can sometimes produce self-dsRNA capable of triggering innate immune responses. For instance, self-dsRNA is produced by transcription of repetitive DNA elements in the genome in response to promoter hypomethylation.[10,42] In addition, genetic deficiency

of the dsRNA-editing enzyme ADAR1 leads to accumulation of host dsRNA.[43] In both instances, there is activation of the 2-5A/RNase L pathway. dsRNA principally activates three types of innate immune pathways: (1) upon sensing dsRNA, RIG-I like receptors signal through MAVS to IRF3 and NF-κB to induce transcription of genes for IFNs and other proinflammatory cytokines,[44] (2) the IFN-inducible and dsRNA-dependent protein kinase PKR phosphorylates eIF2α, causing inhibition of most protein syntheses,[45] and (3) dsRNA stimulates OASs to produce a series of unusual 5′-triphosphorylated 2′,5′-linked short oligoadenylates (2-5A) that activate RNase L.[9,12,13,22] By cleaving ssRNA, RNase L can have profound effects on cells. In particular, OAS-RNase L inhibits many types of RNA viruses, including severe acute respiratory syndrome coronavirus 2 (but not Zika virus, where RNase L increases viral replication) and at least one type of DNA virus, the poxvirus vaccinia virus.[11,46–48] RNase L activation beyond a threshold level also causes the infected cells to spiral into apoptosis, preventing further virus replication.[25,49,50] In addition, our study reveals a pathway by which RNase L upregulates transcript levels for proinflammatory genes that typically restrict viral infections.

2-5A/RNase L induced alteration in the host cell transcriptome

In recent years, insight into complex biological processes has been obtained through quantitative and comprehensive examination of the RNA pool in cells (RNA-seq) by next-generation sequencing. Characterizing the host innate immune response to infection by pathogens is one of many areas in which RNA-seq isinformative.[51] Virus infection has profound effects on host cell gene expression owing in part to induction of IFNs and their downstream effects. In addition, the OAS-RNase L pathway is responsible for the rapid degradation of viral and host ssRNA.[20–22,52]

Dissecting effects of RNase L on the transcriptome of virus-infected cells is complicated in part because viruses typically replicate to higher levels in RNase L KO cells than in WT cells.[22,50] Therefore, virus-induced alterations in the transcriptome may be amplified in RNase L KO cells, thus obscuring direct effects of RNase L on RNA levels. For instance, viruses induce type I and III IFNs, which lead to the expression of hundreds of ISG transcripts.[53] An alternative approach to transfecting cells with dsRNA, typically with the synthetic dsRNA pIC as a virus surrogate, has its own fingerprint on the transcriptome. Among the effects of dsRNA are induction of IFNs and other cytokine mRNAs, or their degradation, as well as OAS-RNase L and PKR activation.[45] Therefore, in the present study, we focused on directly and specifically activating RNase L in cells with its natural ligand, 2-5A. In addition, we compared effects of 2-5A and pIC on the ribotoxic stress response pathway.

Different approaches were used to normalize and validate the RT-qPCR data in this study. For mouse BMM samples, RT-qPCR data were normalized with GAPDH mRNA. Alternately, because GAPDH mRNA levels are decreased by RNase L,[20,21] data were also normalized to total levels of input mRNA. For human samples, RT-qPCR data were normalized to SON mRNA, an mRNA that is resistant to RNase L.[21] Furthermore, because small differences in the total RNA content in 2-5A-transfected cells could artificially enlarge the differences for upregulated mRNAs, inhibitors of p38α, JNK, AP-1, and

ZAK were used to confirm 2-5A-induced transcriptional activity. There were the expected decreases in levels of a wide range of different gene transcripts by RNase L-mediated RNA cleavage, but there was also induction of many transcripts for proinflammatory cytokines, chemokines, and transcription factors. These results confirm our prior report of 2-5A-induced upregulation of many proinflammatory mRNA species, including IL-8 (CXCL8), CXCL1, and IL-17R.[33] Our studies are consistent with a ribotoxic stress response in which 2-5A/RNase L signals through ZAKα, MAP2Ks, JNK, and p38α to the AP-1 transcription factor.[25,26] Interestingly, induction of proinflammatory transcripts by 2-5A/RNase L occurs simultaneously with widespread massive degradation of ssRNA. The net accumulation of some proinflammatory mRNAs in response to 2-5A activation of RNase L suggests that for these transcripts, mRNA synthesis rates exceeded degradation rates. The results provide an intriguing level of complexity to the regulation of the transcriptome by RNase L.

Although RNase L cleaves rRNAs and some tRNAs, it is cleavage of mRNAs that is believed to primarily impair protein synthesis.[19–21,23,24] Because rRNA degradation in intact ribosomes by RNase L does not appear to inhibit translation, there may not be an impediment to the translation of the induced mRNAs.[19,21] Accordingly, we previously showed that 2-5A/RNase L-induced transcription of the GDF15 gene resulted in production of the GDF15 protein.[33] The DAP kinase DRAK1 is another 2-5A/RNase L-induced protein.[27] In this study, we show enhanced levels of Fosb, c-Jun, and IL-1β levels in 2-5A-transfected cells.

RNase L activation and the ribotoxic stress response

While precisely how RNase L activity leads to ZAKα activation is unknown, prior studies suggest a mechanism. Activation of ribosome-associated ZAKα occurs in response to ribosome stalling and/or collisions.[4,54] In addition, RNase L cleaves mRNAs internally in actively translating polysomes. That results in translation of alternative open reading frames present in the RNA cleavage products which are derived internally to the coding sequence and in the 5′ and 3′ UTRs.[55] When translating RNAs lack a stop codon, ribosomes do not dissociate, likely resulting in ribosome collisions.[56,57]Accordingly, a potential pathway to ZAKα activation is ribosome collisions on RNase L-mediated RNA cleavage products lacking a stop codon. Ribosome collisions need not be widespread but could be transient and/or local. In this study, while we did observe increased levels of ribosome collisions upon RNase L activation, we are not in a position to conclude that these structures are responsible for all of the observed ribotoxic stress response activation. Collectively, our findings indicate that 2-5A/RNase L activity results in a ZAKα-initiated kinase cascade, which induces proinflammatory transcripts and apoptosis. Future studies on 2-5A/RNase L activation of ZAKα might inform drug development efforts aimed at controlling cancer and virus-mediated inflammation.

Limitations of study

A precise estimate of 2-5A transfection efficiency was not deter-mined. A prior study showed that 90% of A549 cells transfected with pIC activated OAS/RNase L.[20] Therefore, the reduced levels of mRNA degradation in this study compared to prior published data

involving pIC could be due to a lower transfection efficiency with 2-5A. In addition, 2-5A is degraded within minutes by cellular enzymes,[58] whereas stimulation of OAS enzymes by pIC might lead to prolonged 2-5A synthesis. BMMs and cell lines were derived from males, thus limiting the generalizability of conclusions.

STAR★METHODS

RESOURCE AVAILABILITY

Lead contact—Please direct any requests for further information or reagents to the lead contact, Robert Silverman (silverr@ccf.org).

Materials availability—Reagents generated in this study may be available from the lead contact Robert Silverman (silverr@ccf.org) or Jiajia Xi (xij@ccf.org) with a completed Materials Transfer Agreement.

Data and code availability

- Raw sequencing data were deposited in the NCBI GEO database under the accession number GSE253530.
- This paper does not report original code.
- Any additional information required to reanalyze the data reported in this work is available from the lead contact upon request.

EXPERIMENTAL MODEL AND STUDY PARTICIPANT DETAILS

Mice—Wild type (WT) C57BL/6 mice were purchased from The Jackson Laboratory. *Rnasel*$^{-/-}$ (KO) mice were previously generated and back-crossed on a C57BL/6 background.[50,60] Only male mice were used in the study and were 8-to-12 weeks of age. All mouse studies at Cleveland Clinic were performed in compliance with a protocol approved by the Institutional Animal Care and Use Committee of the Cleveland Clinic Lerner Research Institute. ZAK KO mice in C57BL/6 background[54] (male, 10 weeks of age) were housed in the animal facility of the Department of Experimental Medicine at the University of Copenhagen under the oversight of the Institutional Animal Care and Use Committee. All mouse experiments were conducted in compliance with Danish regulations and approved by the Danish Animal Experiments Inspectorate. Mice were maintained on a 12-h light:dark cycle and had unrestricted access to commercial rodent chow and water prior to the experiment.

Cell lines and culture conditions—Human THP-1 monocytic cell line (from an acute monocytic leukemia, male) was cultured in RPMI1640 medium (Media Preparation Core, Lerner Research Institute) supplemented with 10% FBS (Gibco ref. 10437–028 from Thermo Fisher Scientific) and 50 μM of β-mercaptoethanol (Sigma-Aldrich). Human A549 cell line (derived from epithelial cells from a lung of a male with carcinoma) was cultured in RPMI1640 medium supplemented with 10% FBS. *Rnasel* KO of cell lines were made with a CRISPR-cas9 lentivirus generated by transfecting the LentiCRISPR-sgRL-6 [a gift from Dr. Susan Weiss, University of Pennsylvania[11]] or by infecting with control lentivirus obtained

by transfecting vector lentiCRISPR v2, with psPAX2 and pCMV-VSV-G plasmids at 2:1:1 ratio into human kidney 293T epithelial-like cells cultured in DMEM medium (Media Preparation Core, Lerner Research Institute) supplemented with 10% FBS. ZAK knockout THP-1 and A549 cells were made by infecting with a CRISPR-cas9 lentivirus generated by transfecting the LentiCRISPR-sg (containing the gRNA sequence from Vind et al.[3]) or by infecting with control lentivirus as described above. The virus supernatants were harvested 72 h after transfection and passed through a 0.22 μm filter. Infections were done in THP-1 or A549 cells with 1 mL virus supernatant supplemented with 8 μg/mL polybrene. Cells were centrifuged in 6-well plates at 600×g for 2 h and cultured overnight. Subsequently, cells were collected and centrifuged at 300×g for 5 min. Cells were resuspended into RPMI1640 medium (supplemented with 10% FBS) containing puromycin (2 μg/mL) and pipetted into 96-well plates for selection of single colonies. After 4 weeks of selection, surviving colonies were validated by probing Westerns blots for absence of RNase L with monoclonal antibody against human RNase L.[14] MAVS KO and its control A549 cells (all cultured in DMEM with 10% FBS) were described previously and were gifts from Susan R. Weiss (University of Pennsylvania).[43,59]

Bone marrow derived macrophages—Bone marrow cells were isolated from hind limbs of age matched 8- to 12-week-old WT male or *Rnasel*$^{-/-}$ male or *Zak*$^{-/-}$ male mice. After removing the red blood cells with ACK Lysing Buffer, remaining cells were seeded at 4×10^6 cells per well in 6-well plate in 2 mL of DMEM medium supplemented with 10% FBS, 50 μM β-mercaptoethanol and 20 ng/mL recombinant murine M-CSF with medium changed every 2 days. After 7 days of culture, cells were ready for transfection.

METHOD DETAILS

Preparation of 2-5A—Trimer 2-5A (ppp5′A2′p5′A2′p5′A) was enzymatically synthesized from ATP with histidine-tagged porcine OAS1. “2-5A” generally refers to HPLC-purified ppp5′A2′p5′A2′p5′A (Figure S1A), prepared as described previously.[70] “A3” refers to A2′p5′A2′p5′A (Figure S1B), prepared by dephosphorylation of 2-5A as described.[70] “2-5A oligomers” refers to the mixture of 5′-phosphorylated, 2′,5′-oligoadenylates prepared enzymatically[70] (Figure S1E). HPLC analysis in Figures S1A and S1B were with a Poroshell 120 C18 analytical column (Agilent), whereas in Figure S1E, HPLC was with a preparative Dionex column (BioLC DNAPac™ PA-100).[70]

Transfections and treatment of cells for RNA analysis and Western blots—WT or *Rnasel* KO macrophages were pretreated for 1 h with JNK inhibitor (30 μM), p38α inhibitor (30 μM), AP-1 inhibitor (10 μM) or 30 min with ZAK inhibitor [3h (10 μM) or 6p (10 μM)] or IKKα inhibitor BAY11–7082 (5 μM). The pretreated or untreated BMMs or A549 cells were transfected with active trimer 2-5A (2′,5′-p_3A_3), inactive dephosphorylated A3 (2′,5′-A_3)[70] or with pIC at the concentrations indicated in figure legends with Lipofectamine 2000 or Lipofectamine 3000, according to the manufacturer’s instructions. THP-1 cells were transfected with 2-5A in reverse transfection manner adding cells to the lipofectamine/2-5A mixture according to the manufacturer’s instruction, and then seeding cells in 12-well plates. At the indicated time after transfection, cells were harvested either with RIPA buffer for Western blots or with EZ-10 Spin Columns Total

RNA Minipreps Super Kit following the manufacturer's instructions. Anisomycin (5 μM) treatments were done on THP-1 or A549 cells for 1h, and cells were harvested with RIPA buffer for Western blots. Unless stated otherwise in the Figure Legends, all of the Western blots in the same figure panel were from the same experiment, but not necessarily from the same gel.

Separation of cell lysates into cytoplasmic and nuclear fractions—Cell fractionation was done with Thermo Scientific NE-PER Nuclear and Cytoplasmic Extraction Reagents (Catalog Number 78833), following the manufacturer's instructions. The nuclear fraction marker, lamin B, and cytoplasmic marker, α-tubulin, were probed on Western blots as an indication of fractionation efficiency.

rRNA cleavage assays for RNase L activity—After mock transfection or transfections with 2-5A or pIC at the indicated concentrations and times, cells were lysed with RLT buffer and the total RNA was isolated with EZ-10 Spin Columns Total RNA Minipreps Super Kit. RNA was separated on RNA chips with an Agilent Bioanalyzer 2000 and the RNA separation images were obtained.

Polysome profiling—Cells were transfected with 2-5A oligomers (600 μM, ATP equivalents) for 1.5 h using Lipofectamine 3000 as per the manufacturer's instructions. Following treatment, cytosolic lysates were prepared using 20 mM HEPES pH 7.5, 100 mM NaCl, 5 mM $MgCl_2$, 100 μg/mL digitonin, 100 μg/mL cycloheximide, 1X protease inhibitor cocktail and 200 U RiboLock RNase Inhibitor. Extracts were pushed 10 times through a 26G needle and incubated on ice for 5 min prior to centrifugation at 17,000 g for 5 min at 4°C. After adding calcium chloride to a final concentration of 1 mM, lysates were digested with 500 U micrococcal nuclease (MNase) for 30 min at 22°C. Digestion was terminated by adding EGTA to 2 mM. The resulting lysates containing 260 mg of MNase-digested RNA were resolved in 15–50% sucrose gradients by centrifugation at 38,000 rpm in a Sorvall TH64.1 rotor for 2.5 h at 4°C. The gradients were analyzed using a Biocomp density gradient fractionation system with continuous monitoring of the absorbance at 260 nm.

Bulk RNA-sequencing (RNAseq)—The WT and Rnasel$^{-/-}$ BMM were mock-transfected or transfected with either 2-5A ($2'–5'p_3A_3$) (20 μM) or as a negative control A3 ($2'–5'A_3$) (20 μM) in RNase-free water in the presence of lipofectamine and incubated for 3 h at 37°C in an incubator with 5% CO_2. RNA was extracted, quantified in a uv spectrophotometer, and evaluated for integrity by RNA chip on an Agilent Bioanalyzer, model 2100. mRNA-Seq libraries were prepared from poly(A) tailed RNA, quantified and sequenced at Novogene. Primary analysis of the RNA-seq data was done at the Bioinformatic Core Facility, Florida Research & Innovation Center, Cleveland Clinic by Adrian Reich, and at the Institute for Computational Biology, School of Medicine, Case Western Reserve University by E. Ricky Chan. Briefly, the RNA-seq original sequence data FASTQ files were first inspected by fastqc to ensure data quality. The reads were trimmed of exogenous adapter sequences and low-quality bases were removed using cutadapt (version 2.8). The trimmed reads were aligned to the mouse genome (ENSEMBL GRCm38). Quantification of reads was performed to generate the gene-level feature counts from the

read alignment with STAR (version 2.7.5a). The feature counts were further normalized for the gene size and library to obtain the gene expression value for all genes and all samples. The differential gene expression analyses were conducted by contrasting the 2-5A- or A3-transfected samples, with the mock-transfected samples by DESeq2 (version 1.30.1) and DEXSeq (version 1.36.0) using R (version 4.0.4). After obtaining the sequence reads and DESeq2 comparison tables (Tables S2–S8), the gene expression data were plotted using volcano plot and heatmap by R program (gene list in heatmaps are shown in Tables S10–S14), and the clustering of genes was based on complete linkage and the Euclidean distances of gene expression values. Gene set enrichment analysis (GSEA) was conducted by projecting the fold-change ranking onto Hallmark gene sets (Table S9) (https://www.gsea-msigdb.org/gsea/msigdb/human/genesets.jsp?collection=H) and C5 ontology gene sets (https://www.gsea-msigdb.org/gsea/msigdb/genesets.jsp? collection = C5).

RT-qPCR—Total RNA was extracted from BMM, THP-1 cells and A549 cells as described above. RNA was reverse transcribed with high-capacity cDNA reverse transcriptase kit (4368814, ThermoFisher). RT-qPCR was performed with oligonucleotide primers (Table S1) and Bullseye EvaGreen qPCR 2x MasterMix-ROX (BEQPCR-R, MidSci) using a BioRad qPCR system (CFX Opus 384). Results were analyzed by the ΔCt or ΔΔCt method, as described in the manufacturer's instructions.

ZAKα gel shift assays—A549 cells were pretreated with ZAK inhibitor compounds 3h (10 μM) or 6p (10 μM) for 30 min. The treated or untreated cells were then transfected with 2-5A (20 μM) for 2 h or treated with anisomycin (5 μM) for 1 h, and total protein was harvested with RIPA buffer. Proteins in cell lysates were separated on 7.5% Phos-Tag SDS-PAGE following the manufacturer's instructions. The gels were then treated with 1 mM EDTA and the protein was transferred to PVDF membrane for Western blotting with anti-ZAKα antibody.

Cell survival assays by real-time imaging of cells—Cells (2×10^4 per well) were seeded in 24 well plates. After 18 h cells were mock transfected or transfected with 2-5A (20 μM) and stained for total cells with Syto 60 red fluorescent nucleic acid stain (250 nM) (converted to blue by IncuCyte software) and for dead cells with Sytox green nucleic acid stain (250 nM) in culture medium, then cells were cultured in an IncuCyte live–cell imaging system (SX5) for 60 h in an incubator at 37°C/5% CO_2. Cell viability was calculated by counting the number of green objects per well (dead cells) which was then normalized to the total number of cells per well (red objects) and the averages of 9–16 images were presented as the final data.

QUANTIFICATION AND STATISTICAL ANALYSIS

Statistical analysis—Details of statistical methods, including numbers of biological and technical replicates (n values), and p values, are included in the figure legends. GraphPad Prism 5 software was used for unpaired t-tests and two-way ANOVA. For RNAseq data, differential gene expression (DEG) analysis was done with DESeq2 (version 1. 30.1) and

DEXSeq (version 1.36.0) using R (version 4.0.4). No methods were used to determine whether the data met assumptions of the statistical approach.

Supplementary Material

Refer to Web version on PubMed Central for supplementary material.

ACKNOWLEDGMENTS

We thank E. Ricky Chan (Case Western Reserve University) and Adrian Reich (Florida Research and Innovation Center, Cleveland Clinic) for primary analysis of RNA-seq data, Xiaoyun Lu (Jinan University, Guangzhou) for the generous gift of ZAKis, George Stark (Cleveland Clinic) and Bill Merrick (Case Western Reserve University) for discussions, and Susan R. Weiss (University of Pennsylvania) for gifts of CRISPR constructs and cell lines. The graphical abstract illustration is by David Schumick, BS, CMI, and was reprinted with permission, Cleveland Clinic Foundation copyright 2024, all rights reserved. This research was supported by the National Institute of Allergy and Infectious Diseases of the National Institutes of Health under awards R01 AI135922 (to R.H.S.) and R01 AI104887 (to R.H.S and Susan R. Weiss). Work in the Bekker-Jensen lab was supported by the European Research Council under the European Union's Horizon 2020 research and innovation programme (grant agreement 863911 - PHYRIST). The Center for Gene Expression (CGEN) is a Center of Excellence funded by the National Danish Research Foundation (grant no. DNRF166).

REFERENCES

1. Vind AC, Genzor AV, and Bekker-Jensen S (2020). Ribosomal stress-surveillance: three pathways is a magic number. Nucleic Acids Res. 48, 10648–10661. 10.1093/nar/gkaa757. [PubMed: 32941609]
2. Iordanov MS, Pribnow D, Magun JL, Dinh TH, Pearson JA, Chen SL, and Magun BE (1997). Ribotoxic stress response: activation of the stress-activated protein kinase JNK1 by inhibitors of the peptidyl transferase reaction and by sequence-specific RNA damage to the alpha-sarcin/ricin loop in the 28S rRNA. Mol. Cell Biol. 17, 3373–3381. 10.1128/MCB.17.6.3373. [PubMed: 9154836]
3. Vind AC, Snieckute G, Blasius M, Tiedje C, Krogh N, Bekker-Jensen DB, Andersen KL, Nordgaard C, Tollenaere MAX, Lund AH, et al. (2020). ZAKalpha Recognizes Stalled Ribosomes through Partially Redundant Sensor Domains. Mol. Cell 78, 700–713. 10.1016/j.molcel.2020.03.021. [PubMed: 32289254]
4. Wu CCC, Peterson A, Zinshteyn B, Regot S, and Green R (2020). Ribosome Collisions Trigger General Stress Responses to Regulate Cell Fate. Cell 182, 404–416.e14. 10.1016/j.cell.2020.06.006. [PubMed: 32610081]
5. Iordanov MS, Pribnow D, Magun JL, Dinh TH, Pearson JA, and Magun BE (1998). Ultraviolet radiation triggers the ribotoxic stress response in mammalian cells. J. Biol. Chem. 273, 15794–15803. 10.1074/jbc.273.25.15794. [PubMed: 9624179]
6. Wang X, Mader MM, Toth JE, Yu X, Jin N, Campbell RM, Small-wood JK, Christe ME, Chatterjee A, Goodson T Jr., et al. (2005). Complete inhibition of anisomycin and UV radiation but not cytokine induced JNK and p38 activation by an aryl-substituted dihydropyrrolopyrazole quinoline and mixed lineage kinase 7 small interfering RNA. J. Biol. Chem. 280, 19298–19305. 10.1074/jbc.M413059200. [PubMed: 15737997]
7. Sauter KAD, Magun EA, Iordanov MS, and Magun BE (2010). ZAK is required for doxorubicin, a novel ribotoxic stressor, to induce SAPK activation and apoptosis in HaCaT cells. Cancer Biol. Ther. 10, 258–266. 10.4161/cbt.10.3.12367. [PubMed: 20559024]
8. Zhou A, Hassel BA, and Silverman RH (1993). Expression cloning of 2-5A-dependent RNAase: a uniquely regulated mediator of interferon action. Cell 72, 753–765. 10.1016/0092-8674(93)90403-d. [PubMed: 7680958]
9. Hovanessian AG, Brown RE, and Kerr IM (1977). Synthesis of low molecular weight inhibitor of protein synthesis with enzyme from interferon-treated cells. Nature 268, 537–540. 10.1038/268537a0. [PubMed: 560630]
10. Banerjee S, Gusho E, Gaughan C, Dong B, Gu X, Holvey-Bates E, Talukdar M, Li Y, Weiss SR, Sicheri F, et al. (2019). OAS-RNase L innate immune pathway mediates the

cytotoxicity of a DNA-demethylating drug. Proc. Natl. Acad. Sci. USA 116, 5071–5076. 10.1073/pnas.1815071116. [PubMed: 30814222]

11. Li Y, Banerjee S, Wang Y, Goldstein SA, Dong B, Gaughan C, Silverman RH, and Weiss SR (2016). Activation of RNase L is dependent on OAS3 expression during infection with diverse human viruses. Proc. Natl. Acad. Sci. USA 113, 2241–2246. 10.1073/pnas.1519657113. [PubMed: 26858407]
12. Kerr IM, and Brown RE (1978). pppA2'p5'A2'p5'A: an inhibitor of protein synthesis synthesized with an enzyme fraction from interferon-treated cells. Proc. Natl. Acad. Sci. USA 75, 256–260. 10.1073/pnas.75.1.256. [PubMed: 272640]
13. Kristiansen H, Gad HH, Eskildsen-Larsen S, Despres P, and Hartmann R (2011). The oligoadenylate synthetase family: an ancient protein family with multiple antiviral activities. J. Interferon Cytokine Res. 31, 41–47. 10.1089/jir.2010.0107. [PubMed: 21142819]
14. Dong B, and Silverman RH (1995). 2-5A-dependent RNase molecules dimerize during activation by 2-5A. J. Biol. Chem. 270, 4133–4137. 10.1074/jbc.270.8.4133. [PubMed: 7876164]
15. Huang H, Zeqiraj E, Dong B, Jha BK, Duffy NM, Orlicky S, Thevakumaran N, Talukdar M, Pillon MC, Ceccarelli DF, et al. (2014). Dimeric structure of pseudokinase RNase L bound to 2-5A reveals a basis for interferon-induced antiviral activity. Mol. Cell 53, 221–234. 10.1016/j.molcel.2013.12.025. [PubMed: 24462203]
16. Han Y, Donovan J, Rath S, Whitney G, Chitrakar A, and Korennykh A (2014). Structure of human RNase L reveals the basis for regulated RNA decay in the IFN response. Science 343, 1244–1248. 10.1126/science.1249845. [PubMed: 24578532]
17. Clemens MJ, and Williams BR (1978). Inhibition of cell-free protein synthesis by pppA2'p5'A2'p5'A: a novel oligonucleotide synthesized by interferon-treated L cell extracts. Cell 13, 565–572. 10.1016/0092-8674(78)90329-x. [PubMed: 657268]
18. Wreschner DH, McCauley JW, Skehel JJ, and Kerr IM (1981). Interferon action–sequence specificity of the ppp(A2'p)nA-dependent ribonuclease. Nature 289, 414–417. 10.1038/289414a0. [PubMed: 6162102]
19. Donovan J, Rath S, Kolet-Mandrikov D, and Korennykh A (2017). Rapid RNase L-driven arrest of protein synthesis in the dsRNA response without degradation of translation machinery. RNA 23, 1660–1671. 10.1261/rna.062000.117. [PubMed: 28808124]
20. Burke JM, Moon SL, Matheny T, and Parker R (2019). RNase L Re-programs Translation by Widespread mRNA Turnover Escaped by Antiviral mRNAs. Mol. Cell 75, 1203–1217.e5. 10.1016/j.molcel.2019.07.029. [PubMed: 31494035]
21. Rath S, Prangley E, Donovan J, Demarest K, Wingreen NS, Meir Y, and Korennykh A (2019). Concerted 2-5A-Mediated mRNA Decay and Transcription Reprogram Protein Synthesis in the dsRNA Response. Mol. Cell 75, 1218–1228.e6. 10.1016/j.molcel.2019.07.027. [PubMed: 31494033]
22. Silverman RH (2007). Viral encounters with 2',5'-oligoadenylate synthetase and RNase L during the interferon antiviral response. J. Virol. 81, 12720–12729. 10.1128/JVI.01471-07. [PubMed: 17804500]
23. Wreschner DH, James TC, Silverman RH, and Kerr IM (1981). Ribosomal RNA cleavage, nuclease activation and 2-5A(ppp(A2'p)nA) in interferon-treated cells. Nucleic Acids Res. 9, 1571–1581. 10.1093/nar/9.7.1571. [PubMed: 6164990]
24. Silverman RH, Skehel JJ, James TC, Wreschner DH, and Kerr IM (1983). rRNA cleavage as an index of ppp(A2'p)nA activity in interferon-treated encephalomyocarditis virus-infected cells. J. Virol. 46, 1051–1055. 10.1128/JVI.46.3.1051-1055.1983. [PubMed: 6190010]
25. Li G, Xiang Y, Sabapathy K, and Silverman RH (2004). An apoptotic signaling pathway in the interferon antiviral response mediated by RNase L and c-Jun NH2-terminal kinase. J. Biol. Chem. 279, 1123–1131. 10.1074/jbc.M305893200. [PubMed: 14570908]
26. Iordanov MS, Paranjape JM, Zhou A, Wong J, Williams BR, Meurs EF, Silverman RH, and Magun BE (2000). Activation of p38 mitogen-activated protein kinase and c-Jun NH(2)-terminal kinase by double-stranded RNA and encephalomyocarditis virus: involvement of RNase L, protein kinase R, and alternative pathways. Mol. Cell Biol. 20, 617–627. 10.1128/MCB.20.2.617-627.2000. [PubMed: 10611240]

27. Manivannan P, Reddy V, Mukherjee S, Clark KN, and Malathi K (2019). RNase L Induces Expression of A Novel Serine/Threonine Protein Kinase, DRAK1, to Promote Apoptosis. Int. J. Mol. Sci. 20, 3535. 10.3390/ijms20143535. [PubMed: 31330998]
28. Banerjee S, Chakrabarti A, Jha BK, Weiss SR, and Silverman RH (2014). Cell-type-specific effects of RNase L on viral induction of beta interferon. mBio 5, e00856–e00814. 10.1128/mBio.00856-14. [PubMed: 24570368]
29. Chakrabarti A, Banerjee S, Franchi L, Loo YM, Gale M Jr., Núñez G, and Silverman RH (2015). RNase L activates the NLRP3 inflammasome during viral infections. Cell Host Microbe 17, 466–477. 10.1016/j.chom.2015.02.010. [PubMed: 25816776]
30. Chang Y, Lu X, Shibu MA, Dai YB, Luo J, Zhang Y, Li Y, Zhao P, Zhang Z, Xu Y, et al. (2017). Structure Based Design of N-(3-((1H-Pyrazolo[3,4-b]pyridin-5-yl)ethynyl)benzenesulfonamides as Selective Leucine-Zipper and Sterile-alpha Motif Kinase (ZAK) Inhibitors. J. Med. Chem. 60, 5927–5932. 10.1021/acs.jmedchem.7b00572. [PubMed: 28586211]
31. Glazko G, and Mushegian A (2010). Measuring gene expression divergence: the distance to keep. Biol. Direct 5, 51. 10.1186/1745-6150-5-51. [PubMed: 20691088]
32. Li XL, Boyanapalli M, Weihua X, Kalvakolanu DV, and Hassel BA (1998). Induction of interferon synthesis and activation of interferon-stimulated genes by liposomal transfection reagents. J. Interferon Cytokine Res. 18, 947–952. 10.1089/jir.1998.18.947. [PubMed: 9858316]
33. Malathi K, Paranjape JM, Bulanova E, Shim M, Guenther-Johnson JM, Faber PW, Eling TE, Williams BRG, and Silverman RH (2005). A transcriptional signaling pathway in the IFN system mediated by 2'–5'-oligoadenylate activation of RNase L. Proc. Natl. Acad. Sci. USA 102, 14533–14538. 10.1073/pnas.0507551102. [PubMed: 16203993]
34. Sadler AJ, and Williams BRG (2008). Interferon-inducible antiviral effectors. Nat. Rev. Immunol. 8, 559–568. 10.1038/nri2314. [PubMed: 18575461]
35. Loo YM, and Gale M Jr. (2011). Immune signaling by RIG-I-like receptors. Immunity 34, 680–692. 10.1016/j.immuni.2011.05.003. [PubMed: 21616437]
36. Malathi K, Dong B, Gale M Jr., and Silverman RH (2007). Small self-RNA generated by RNase L amplifies antiviral innate immunity. Nature 448, 816–819. 10.1038/nature06042. [PubMed: 17653195]
37. Ye N, Ding Y, Wild C, Shen Q, and Zhou J (2014). Small molecule inhibitors targeting activator protein 1 (AP-1). J. Med. Chem. 57, 6930–6948. 10.1021/jm5004733. [PubMed: 24831826]
38. Hanahan D, and Weinberg RA (2011). Hallmarks of cancer: the next generation. Cell 144, 646–674. 10.1016/j.cell.2011.02.013. [PubMed: 21376230]
39. Yang J, Shibu MA, Kong L, Luo J, BadrealamKhan F, Huang Y, Tu ZC, Yun CH, Huang CY, Ding K, and Lu X (2020). Design, Synthesis, and Structure-Activity Relationships of 1,2,3-Triazole Benzenesulfonamides as New Selective Leucine-Zipper and Sterile-alpha Motif Kinase (ZAK) Inhibitors. J. Med. Chem. 63, 2114–2130. 10.1021/acs.jmedchem.9b00664. [PubMed: 31244114]
40. Burke JM, Gilchrist AR, Sawyer SL, and Parker R (2021). RNase L limits host and viral protein synthesis via inhibition of mRNA export. Sci. Adv. 7, eabh2479. 10.1126/sciadv.abh2479. [PubMed: 34088676]
41. Burke JM, Ripin N, Ferretti MB, St Clair LA, Worden-Sapper ER, Salgado F, Sawyer SL, Perera R, Lynch KW, and Parker R (2022). RNase L activation in the cytoplasm induces aberrant processing of mRNAs in the nucleus. PLoS Pathog. 18, e1010930. 10.1371/journal.ppat.1010930. [PubMed: 36318584]
42. Leonova KI, Brodsky L, Lipchick B, Pal M, Novototskaya L, Chenchik AA, Sen GC, Komarova EA, and Gudkov AV (2013). p53 cooperates with DNA methylation and a suicidal interferon response to maintain epigenetic silencing of repeats and noncoding RNAs. Proc. Natl. Acad. Sci. USA 110, E89–E98. 10.1073/pnas.1216922110. [PubMed: 23236145]
43. Li Y, Banerjee S, Goldstein SA, Dong B, Gaughan C, Rath S, Donovan J, Korennykh A, Silverman RH, and Weiss SR (2017). Ribonuclease L mediates the cell-lethal phenotype of the double-stranded RNA editing enzyme ADAR1 in a human cell line. Elife 6, e25687. 10.7554/eLife.25687. [PubMed: 28362255]
44. Johnson CL, and Gale M Jr. (2006). CARD games between virus and host get a new player. Trends Immunol. 27, 1–4. 10.1016/j.it.2005.11.004. [PubMed: 16309964]

45. Sadler AJ, and Williams BRG (2007). Structure and function of the protein kinase R. Curr. Top. Microbiol. Immunol. 316, 253–292. 10.1007/978-3-540-71329-6_13. [PubMed: 17969452]
46. Li Y, Renner DM, Comar CE, Whelan JN, Reyes HM, Cardenas-Diaz FL, Truitt R, Tan LH, Dong B, Alysandratos KD, et al. (2021). SARS-CoV-2 induces double-stranded RNA-mediated innate immune responses in respiratory epithelial-derived cells and cardiomyocytes. Proc. Natl. Acad. Sci. USA 118, e2022643118. 10.1073/pnas.2022643118. [PubMed: 33811184]
47. Whelan JN, Parenti NA, Hatterschide J, Renner DM, Li Y, Reyes HM, Dong B, Perez ER, Silverman RH, and Weiss SR (2021). Zika virus employs the host antiviral RNase L protein to support replication factory assembly. Proc. Natl. Acad. Sci. USA 118, e2101713118. 10.1073/pnas.2101713118. [PubMed: 34031250]
48. Whelan JN, Li Y, Silverman RH, and Weiss SR (2019). Zika Virus Production Is Resistant to RNase L Antiviral Activity. J. Virol. 93, e00313–19. 10.1128/JVI.00313-19. [PubMed: 31142667]
49. Castelli JC, Hassel BA, Wood KA, Li XL, Amemiya K, Dalakas MC, Torrence PF, and Youle RJ (1997). A study of the interferon antiviral mechanism: apoptosis activation by the 2-5A system. J. Exp. Med. 186, 967–972. 10.1084/jem.186.6.967. [PubMed: 9294150]
50. Zhou A, Paranjape J, Brown TL, Nie H, Naik S, Dong B, Chang A, Trapp B, Fairchild R, Colmenares C, and Silverman RH (1997). Interferon action and apoptosis are defective in mice devoid of 2',5'-oligoadenylate-dependent RNase L. EMBO J. 16, 6355–6363. 10.1093/emboj/16.21.6355. [PubMed: 9351818]
51. Cao Y, Xu X, Kitanovski S, Song L, Wang J, Hao P, and Hoffmann D (2021). Comprehensive Comparison of RNA-Seq Data of SARS-CoV-2, SARS-CoV and MERS-CoV Infections: Alternative Entry Routes and Innate Immune Responses. Front. Immunol. 12, 656433. 10.3389/fimmu.2021.656433. [PubMed: 34122413]
52. Lee D, Le Pen J, Yatim A, Dong B, Aquino Y, Ogishi M, Pescarmona R, Talouarn E, Rinchai D, Zhang P, et al. (2023). Inborn errors of OAS-RNase L in SARS-CoV-2-related multisystem inflammatory syndrome in children. Science 379, eabo3627. 10.1126/science.abo3627. [PubMed: 36538032]
53. Der SD, Zhou A, Williams BR, and Silverman RH (1998). Identification of genes differentially regulated by interferon alpha, beta, or gamma using oligonucleotide arrays. Proc. Natl. Acad. Sci. USA 95, 15623–15628. 10.1073/pnas.95.26.15623. [PubMed: 9861020]
54. Snieckute G, Genzor AV, Vind AC, Ryder L, Stoneley M, Chamois S, Dreos R, Nordgaard C, Sass F, Blasius M, et al. (2022). Ribosome stalling is a signal for metabolic regulation by the ribotoxic stress response. Cell Metabol. 34, 2036–2046.e8. 10.1016/j.cmet.2022.10.011.
55. Karasik A, Jones GD, DePass AV, and Guydosh NR (2021). Activation of the antiviral factor RNase L triggers translation of non-coding mRNA sequences. Nucleic Acids Res. 49, 6007–6026. 10.1093/nar/gkab036. [PubMed: 33556964]
56. Nilsson I, Lara P, Hessa T, Johnson AE, von Heijne G, and Karamyshev AL (2015). The code for directing proteins for translocation across ER membrane: SRP cotranslationally recognizes specific features of a signal sequence. J. Mol. Biol. 427, 1191–1201. 10.1016/j.jmb.2014.06.014. [PubMed: 24979680]
57. Guydosh NR, Kimmig P, Walter P, and Green R (2017). Regulated Ire1-dependent mRNA decay requires no-go mRNA degradation to maintain endoplasmic reticulum homeostasis in S. pombe. Elife 6, e29216. 10.7554/eLife.29216. [PubMed: 28945192]
58. Silverman RH, Wreschner DH, Gilbert CS, and Kerr IM (1981). Synthesis, characterization and properties of ppp(A2'p)nApCp and related high-specific-activity 32P-labelled derivatives of ppp(A2'p)nA. Eur. J. Biochem. 115, 79–85. 10.1111/j.1432-1033.1981.tb06200.x. [PubMed: 7227373]
59. Roth-Cross JK, Martínez-Sobrido L, Scott EP, García-Sastre A, and Weiss SR (2007). Inhibition of the alpha/beta interferon response by mouse hepatitis virus at multiple levels. J. Virol. 81, 7189–7199. 10.1128/JVI.00013-07. [PubMed: 17459917]
60. Leitner WW, Hwang LN, deVeer MJ, Zhou A, Silverman RH, Williams BRG, Dubensky TW, Ying H, and Restifo NP (2003). Alphavirus-based DNA vaccine breaks immunological tolerance by activating innate antiviral pathways. Nat. Med. 9, 33–39. 10.1038/nm813. [PubMed: 12496961]

61. Sanjana NE, Shalem O, and Zhang F (2014). Improved vectors and genome-wide libraries for CRISPR screening. Nat. Med. 11, 783–784. 10.1038/nmeth.3047.

62. Stewart SA, Dykxhoorn DM, Palliser D, Mizuno H, Yu EY, An DS, Sabatini DM, Chen IS, Hahn WC, Sharp PA, et al. (2003). Lentivirus-delivered stable gene silencing by RNAi in primary cells. RNA 9, 493–501. 10.1261/rna.2192803. [PubMed: 12649500]

63. Martin M (2011). Cutadapt removes adapter sequences from high-throughput sequencing reads, 17, p. 3. 10.14806/ej.17.1.200.

64. Dobin A, Davis CA, Schlesinger F, Drenkow J, Zaleski C, Jha S, Batut P, Chaisson M, and Gingeras TR (2013). STAR: ultrafast universal RNA-seq aligner. Bioinformatics 29, 15–21. 10.1093/bioinformatics/bts635. [PubMed: 23104886]

65. Love MI, Huber W, and Anders S (2014). Moderated estimation of fold change and dispersion for RNA-seq data with DESeq2. Genome Biol 15, 550. 10.1186/s13059-014-0550-8. [PubMed: 25516281]

66. Anders S, Reyes A, and Huber W (2012). Detecting differential usage of exons from RNA-seq data. Genome Res 22, 2008–2017. 10.1101/gr.133744.111. [PubMed: 22722343]

67. Reyes A, Anders S, Weatheritt RJ, Gibson TJ, Steinmetz LM, and Huber W (2013). Drift and conservation of differential exon usage across tissues in primate species. Proc. Natl. Acad. Sci. USA 110, 15377–15382. 10.1073/pnas.1307202110. [PubMed: 24003148]

68. Subramanian A, Tamayo P, Mootha VK, Mukherjee S, Ebert BL, Gillette MA, Paulovich A, Pomeroy SL, Golub TR, Lander ES, and Mesirov JP (2005). Gene set enrichment analysis: a knowledge-based approach for interpreting genome-wide expression profiles. Proc. Natl. Acad. Sci. USA 102, 15545–15550. 10.1073/pnas.0506580102. [PubMed: 16199517]

69. Mootha VK, Lindgren CM, Eriksson KF, Subramanian A, Sihag S, Lehar J, Puigserver P, Carlsson E, Ridderstrale M, Laurila E, et al. (2003). PGC-1alpha-responsive genes involved in oxidative phosphorylation are coordinately downregulated in human diabetes. Nat Genet 34, 267–273. 10.1038/ng1180. [PubMed: 12808457]

70. Asthana A, Gaughan C, Dong B, Weiss SR, and Silverman RH (2021). Specificity and Mechanism of Coronavirus, Rotavirus, and Mammalian Two-Histidine Phosphoesterases That Antagonize Antiviral Innate Immunity. mBio 12, e0178121. 10.1128/mBio.01781-21. [PubMed: 34372695]

Highlights

- RNase L activation leads to a ribotoxic stress response
- The stress response requires the ribosome-associated MAP3K ZAKα
- Phosphorylation of ZAKα, MAP2Ks, JNK, and p38α leads to induction of proinflammatory genes
- The stress response triggered by RNase L culminates in apoptosis

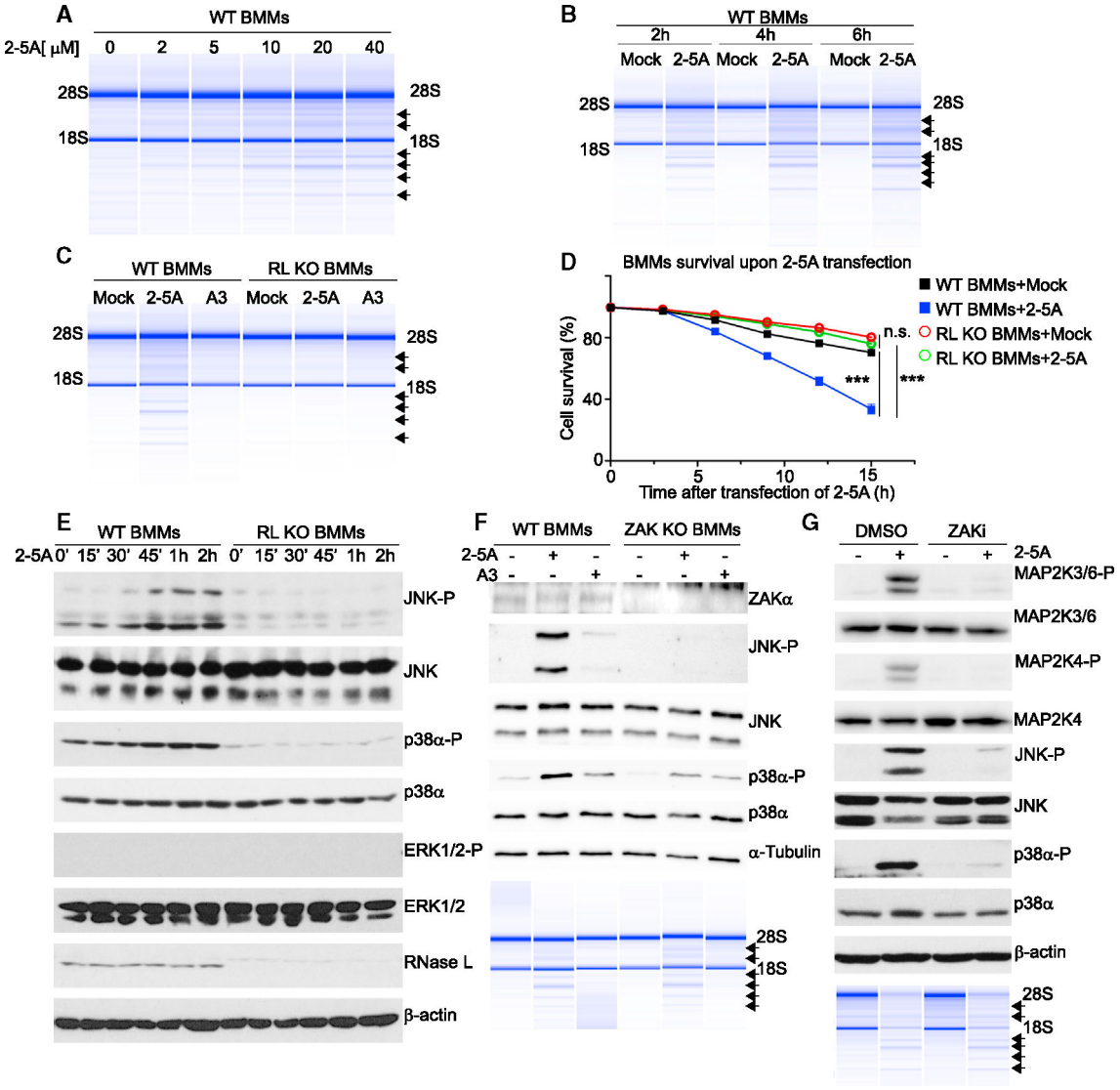

Figure 1. Activation of RNase L by 2-5A in BMMs leads to ZAKα-dependent MAP2K and SAPK phosphorylation and cell death

(A and B) Dose- (A) and time (B)-dependent induction of RNase L activity by 2-5A in WT BMMs as determined by rRNA cleavages.

(C) RNase L mediated rRNA cleavage in WT BMMs, but not in RNase L KO BMMs, by transfection with 2-5A (20 μM) for 3 h in comparison to mock- or A3-transfected controls.

(D) Cell survival as determined by real-time imaging of stained WT or RNase L KO BMMs that were either mock transfected or transfected with 2-5A (20 μM). Data are shown as the mean ± standard error of the mean (SEM) from a single experiment with twelve technical replicates. Significance was determined by two-way ANOVA. ***$p < 0.001$; ns, not significant. The data are from one of two biological replicates.

(E) Total and phosphorylated JNK, p38α, and ERK 1/2; RNase L; and β-actin in 2-5A-transfected WT BMMs and RNase L KO BMMs at different times as determined by western blotting. Data shown are from one of three biological replicates.

(F) Levels of ZAKα, total and phosphorylated JNK and p38α, and α-tubulin in WT BMMs and ZAK KO BMMs transfected with 2-5A (20 μM) or A3 (20 μM) for 2 h as determined by western blotting. Bottom, intact and cleaved rRNA as determined in an RNA chip (Agilent). Data shown are from one of four biological replicates.

(G) Levels of total and phosphorylated MAP2K3/MAP2K6, MAP2K4, JNK, p38α, and β-actin in WT BMM treated with DMSO or ZAK inhibitor (ZAKi) compound 3h in either mock-transfected or 2-5A-transfected (20 μM) WT BMMs for 2 h as determined by western blotting. Bottom, intact and cleaved rRNA in an RNA chip (Agilent). Data shown are from one of two biological replicates.

See also Figure S1.

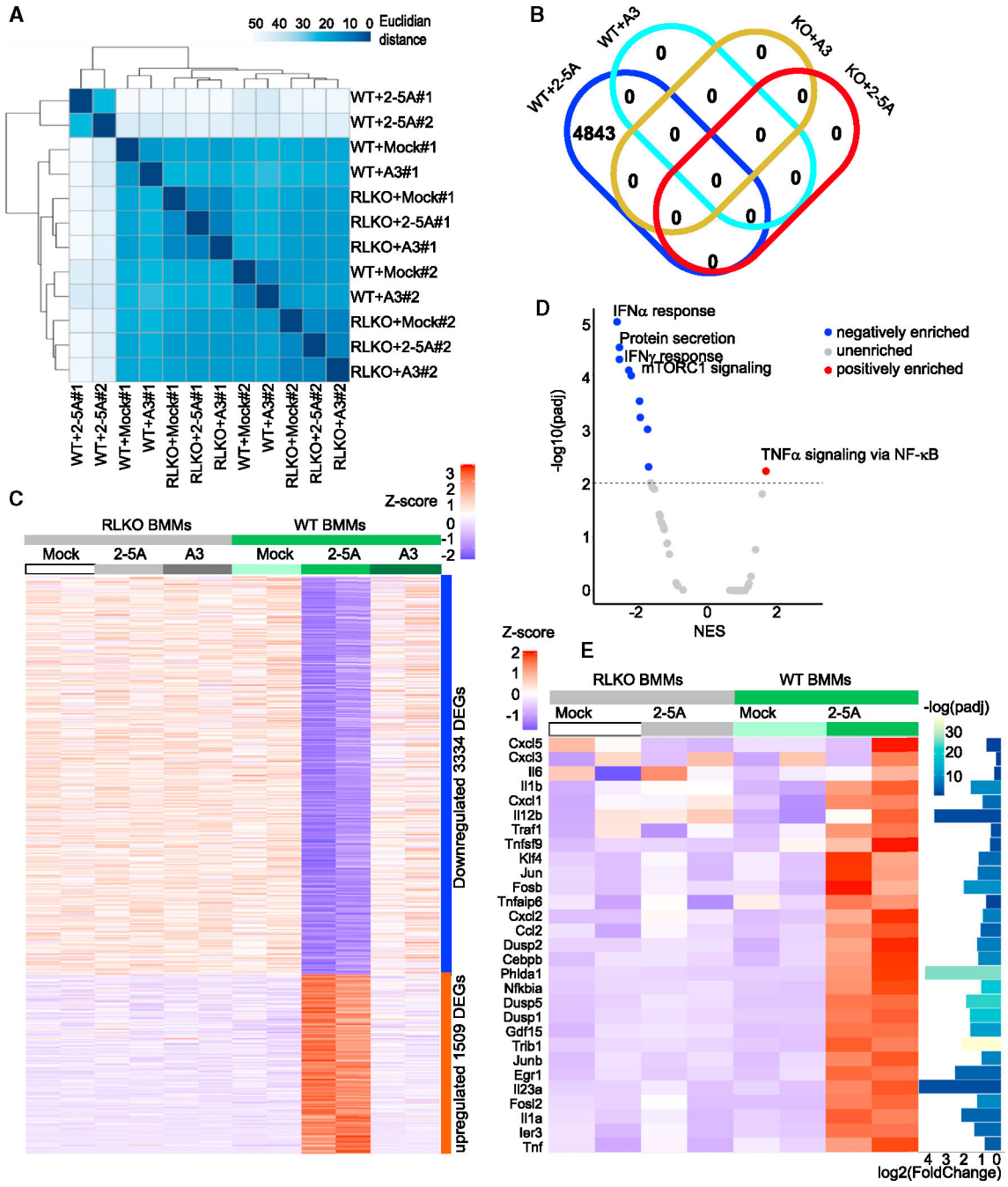

Figure 2. RNase L activation by 2-5A modulates the transcriptome of BMMs, decreasing or increasing levels of different mRNAs

(A) Euclidean distance of gene expression between treatment groups as a measure of sequence divergence.[31] The matrix of distances between each pair of samples is represented by a dendrogram, while the scale of sample-to-sample distances is represented in different shades of blue.

(B) Shared DEGs in mock-, 2-5A-, or A3-transfected WT or RNase L KO BMMs. The Venn diagram depicts transcript changes shared between or unique to each comparison.

(C) Heatmaps of mock-, 2-5A, and A3-transfected WT and RL KO BMMs. The color bar (top right) indicates the Z score.
(D) Volcano plot of 2-5A down- and up-regulated gene sets from WT BMM transcriptomes.
(E) Heatmap of "TNF-α signaling via NF-κB" hallmark gene set from mock- and 2-5A-transfected WT and RL KO BMMs. Insets: Z score (top left) and adjusted p values (padjs) (right inset). RL KO, RNase L KO. There were two biological replicates for each condition in these data.
See also Figures S1–S4.

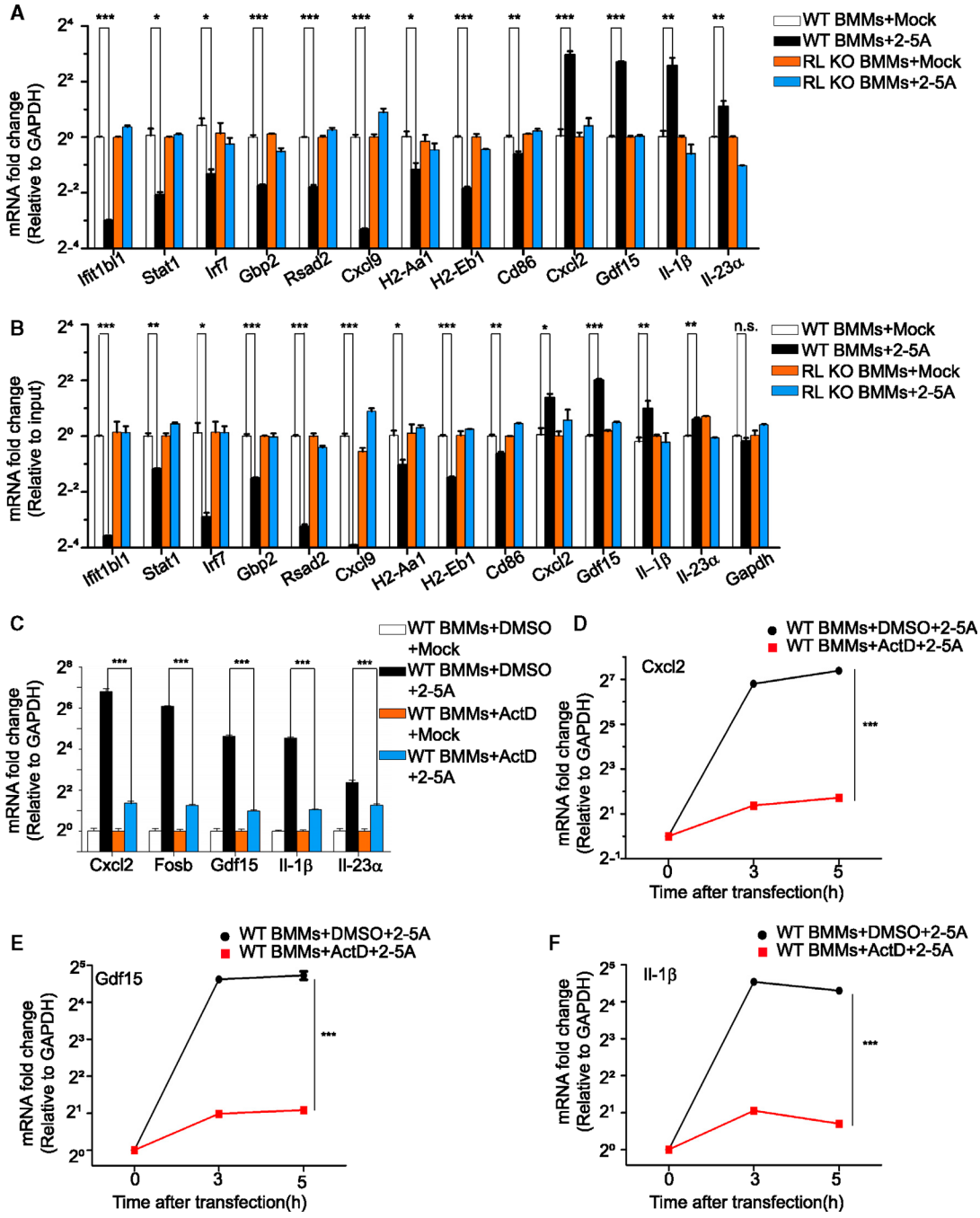

Figure 3. Regulation of transcript levels in mock- or 2-5A-transfected WT and RL KO BMMs

(A and B) Levels of select up- and down-regulated transcripts in mock- and 2-5A-transfected (20 μM for 3 h) WT and RL KO BMMs normalized to (A) GAPDH mRNA levels or (B) input RNA levels as determined by RT-qPCR. Data are shown as the mean ± SEM from a single experiment with three technical replicates. There were two biological replicates with three technical replicates each.

(C–F) Actinomycin D inhibited 2-5A induction (20 μM for 3 h) of select transcripts in WT BMMs as determined by RT-qPCR. Actinomycin D (5 μg per mL) or DMSO was added to

cells 30 min prior to transfections. Relative transcript levels were monitored by RT-qPCR. Data are shown as the mean ± SEM from a single experiment with three technical replicates. There were two biological replicates with three technical replicates each. Significance was determined by unpaired Student's t test. ***$p < 0.001$, **$p < 0.01$, and *$p < 0.05$. ActD, actinomycin D; RL KO, RNase L KO.

See also Figures S2 and S4.

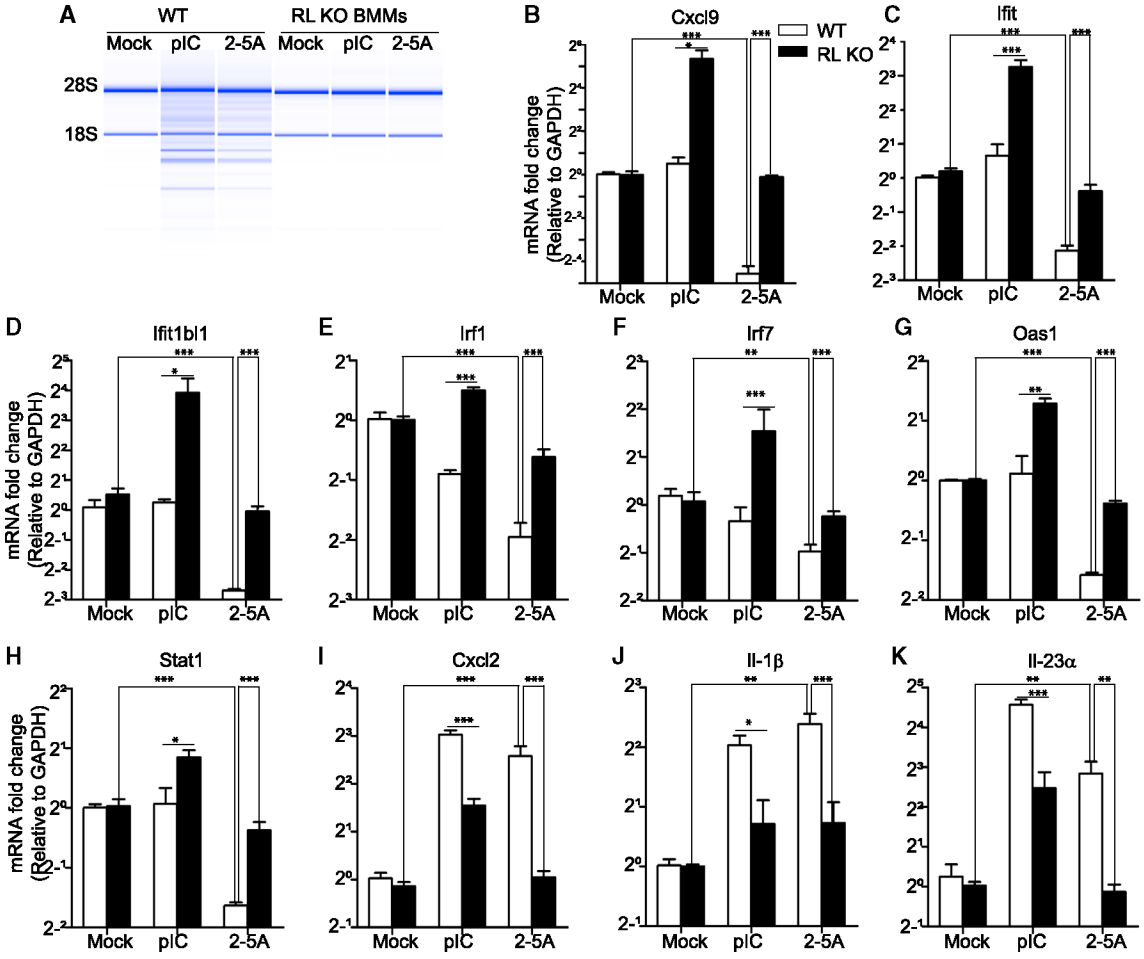

Figure 4. Comparison of representative dsRNA- and 2-5A-induced or -repressed transcripts in BMMs

(A) Cleavage of rRNA in WT BMMs, but not in RNase L KO BMMs, in response to poly(I):poly(C) (pIC) (1 μg per mL, 3 h) or 2-5A (20 μM, 3 h) as determined by analysis on an RNA chip (Agilent).

(B–K) Relative levels of different transcripts (as indicated) with transfection of pIC (1 μg per mL, 3 h) or 2-5A (20 μM, 3 h) as determined by RT-qPCR. Data are shown as the mean ± SEM from a single experiment with three technical replicates. There were two biological replicates with three technical replicates each. ***$p < 0.001$, **$p < 0.01$, and *$p < 0.05$. See also Figures S5 and S7.

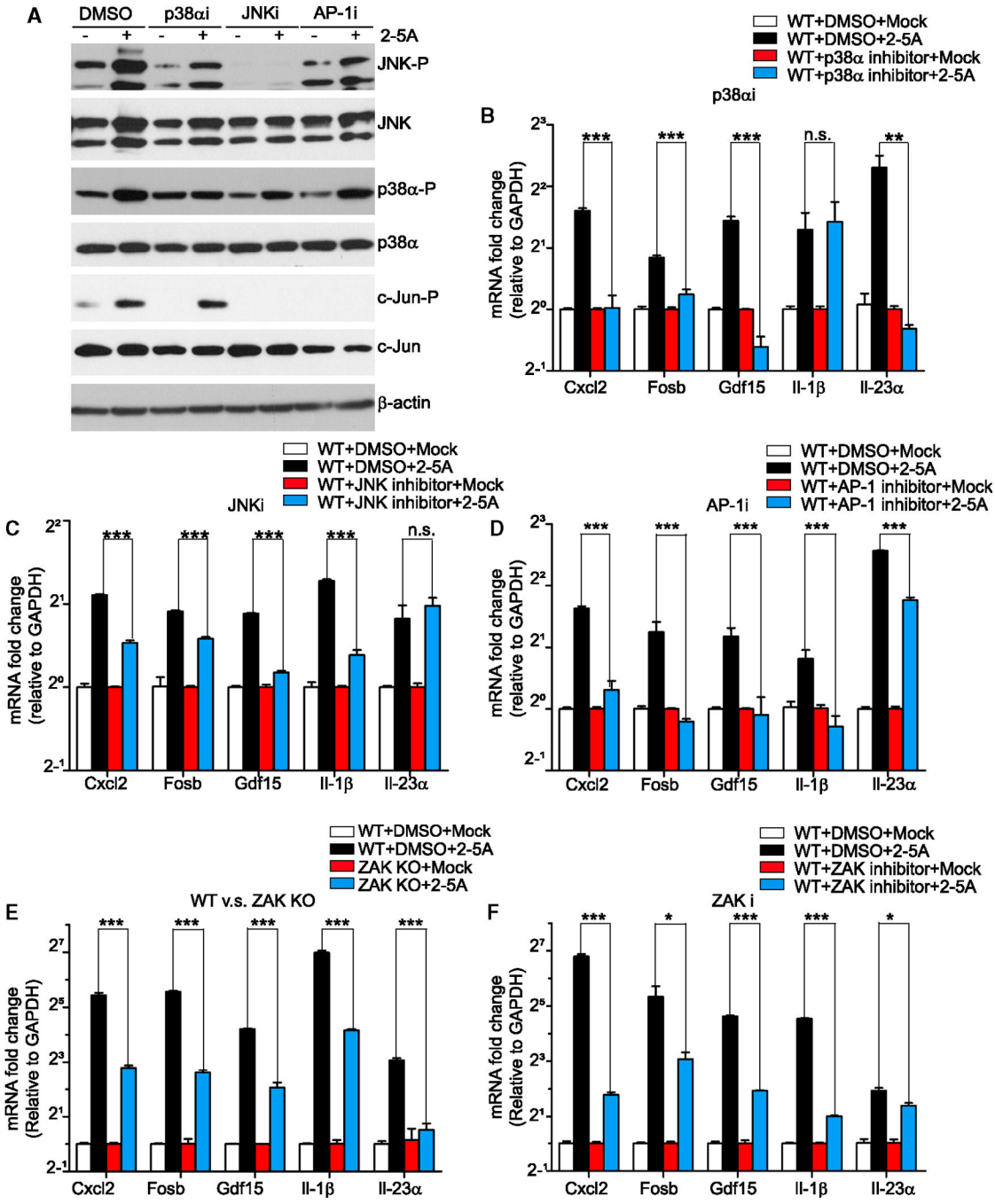

Figure 5. Effects of kinase inhibitors or ZAK KO on protein phosphorylation and/or transcript levels in BMMs following mock or 2-5A transfection

(A) Inhibition of p38α, JNK, and c-Jun phosphorylation by small-molecule inhibitors in 2-5A-transfected WT BMMs as determined by western blotting. Inhibitors, or DMSO, were added to cells for 2 h prior to transfections with 2-5A (20 μM for an additional 3 h). There were two biological replicates.

(B–D) Effects of inhibitors of (B) p38α, (C) JNK, and (D) AP-1 on transcript levels after 2-5A transfection in WT BMMs.

(E) 2-5A induction (20 μM, 3 h) of transcript levels in WT and ZAK KO BMMs.

(F) Effects of ZAKi (compound 3h) on induction of transcript levels in WT BMM.
(B–F) Data are shown as the mean ± SEM from a single experiment with three technical replicates. There were two biological replicates with three technical replicates each. Significance was determined by unpaired Student's t test. ***$p < 0.001$, **$p < 0.01$, and *$p < 0.05$.
See also Figure S5.

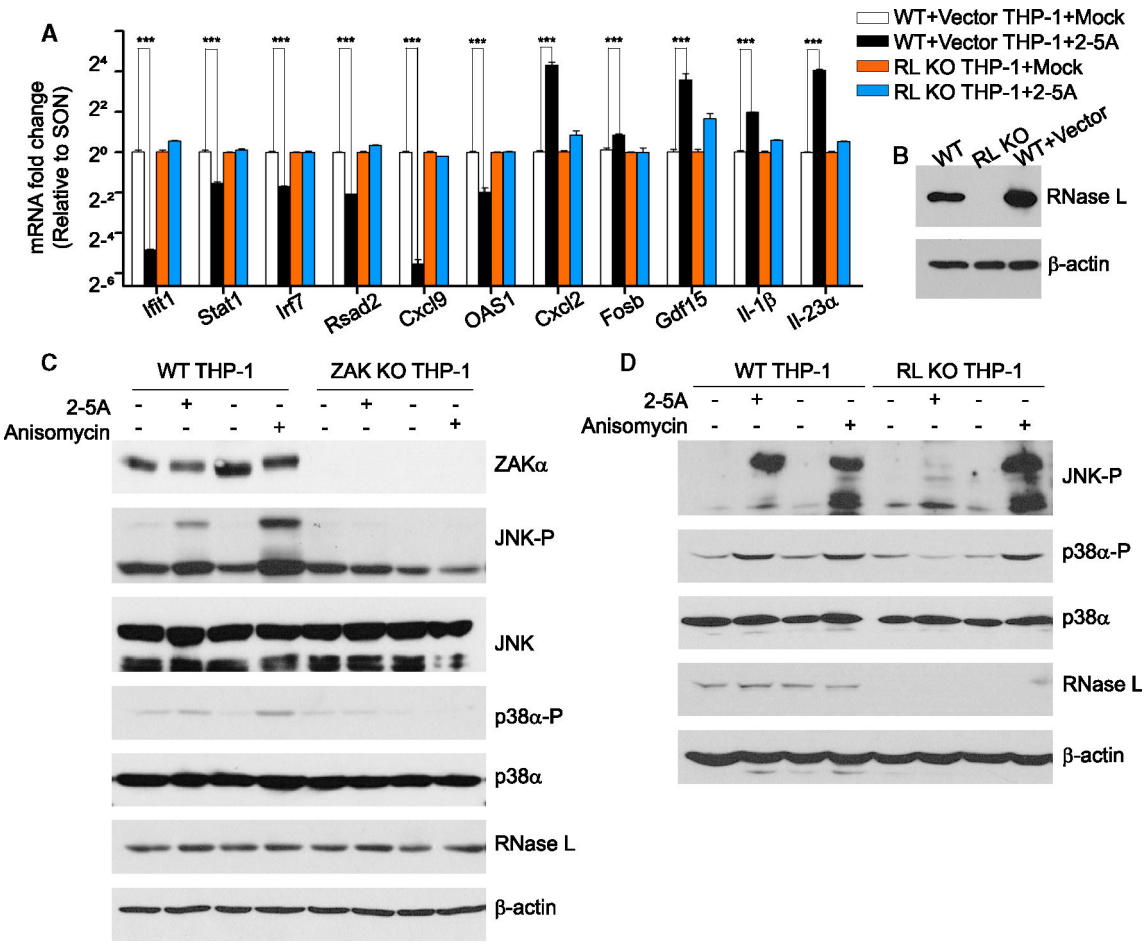

Figure 6. ZAKα is required for the ribotoxic stress response in human THP-1 monocytic cells

(A) Transcript levels in mock- and 2-5A-transfected (20 μM for 3h) WT and RL KO THP-1 cells normalized to SON-DNA- and RNA-binding protein (SON) mRNA levels. Data are shown as the mean ± SEM from a single experiment with three technical replicates. There were two biological replicates with three technical replicates each. Significance was determined by unpaired Student's t test. ***$p < 0.001$.

(B) Western blot of WT, RLKO, and WT vector control THP-1 cells probed with antibody against human RNase L or β-actin. Data show one of two biological replicates.

(C and D) Levels of total or phosphorylated proteins (as indicated) in (C) WT and ZAK KO THP-1 cells or (D) WT and RL KO THP-1 cells that were mock or 2-5A transfected (20 μM, 2 h) or treated with anisomycin (5 μg per mL, 1 h) as determined in western blots. RL KO, RNase L KO. Data shown are from one of two biological replicates.

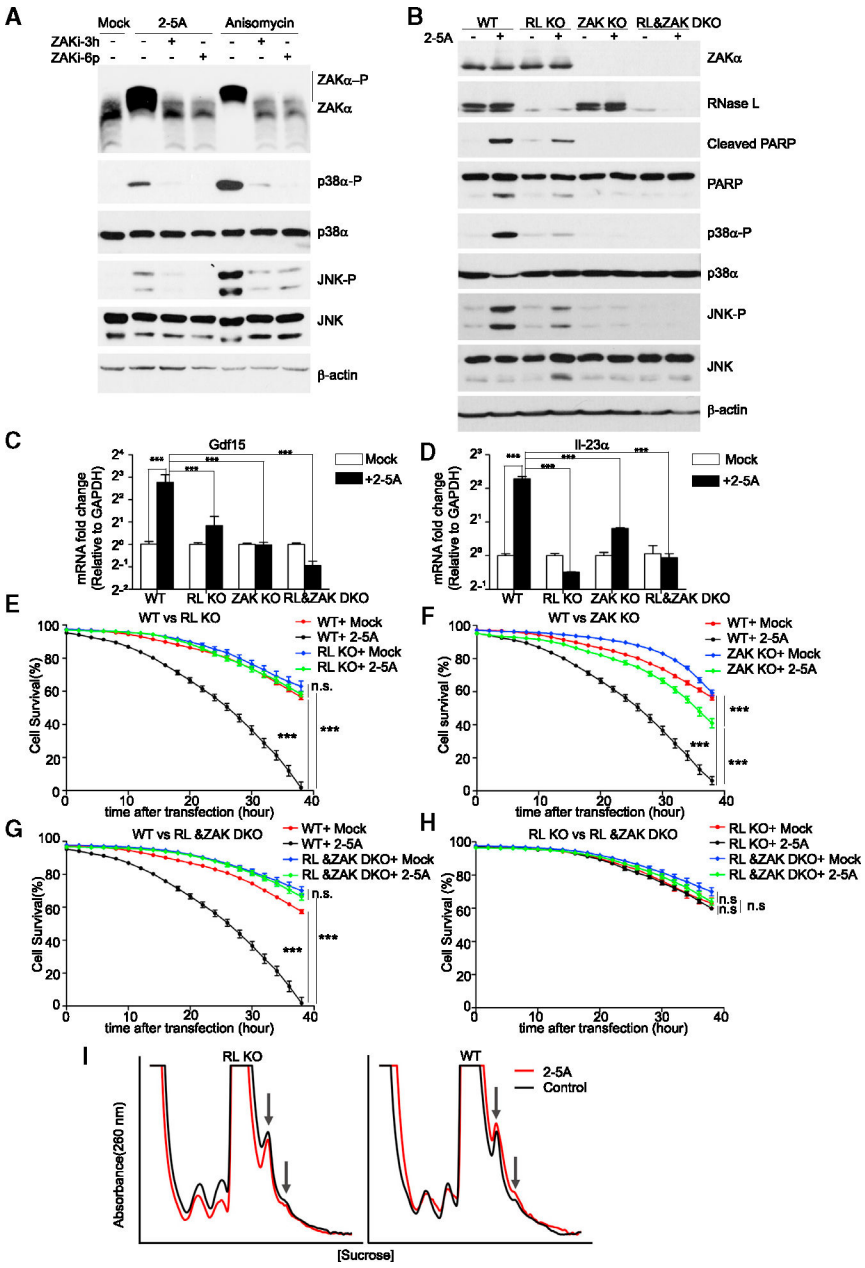

Figure 7. RNase L activity triggers ribosome collisions, ZAKα activation, and apoptosis of A549 cells

(A) ZAKα, p38α, and JNK phosphorylation in WT A549 cells in response to 2-5A transfection (20 μM, 2 h) or anisomycin treatment (5 μg per mL, 1 h) in the presence or absence of ZAKi compounds 3h (10 μM) or 6p (10 μM). Top only: western blot of a Phos-Tag gel probed with antibody against human ZAK was from a separate experiment from the rest of (A). Bottom five images: western blots of standard SDS-PAGE were probed with antibodies against total and phosphorylated p38α and JNK and against β-actin. Data are from one of three biological replicates.

(B) Western blots for total and cleaved PARP and total and phosphorylated p38α and JNK in mock-transfected and 2-5A-transfected (20 μM, 16 h) WT, RL KO, ZAK KO, and RL&ZAK DKO A549 cells. Data are from one of three biological replicates.

(C and D) Levels of (C) GDF15 and (D) IL-23α transcripts relative to GAPDH transcript levels in WT, RL KO, ZAK KO, and RL&ZAK DKO A549 cells fter mock or 2-5A transfection (20 μM, 3 h) as determined by RT-qPCR. Data are shown as the mean ± SEM from a single experiment with three technical replicates. There were two biological replicates with three technical replicates each. Significance was determined by unpaired Student's t tests.

(E–H) Cell survival curves for WT, RL KO, ZAK KO, and RL&ZAK DKO A549 cells (as indicated) that were mock or 2-5A transfected (20 μM 2-5A). For comparisons between different treatment groups, the same reference datasets for WT, RL KO, and RL&ZAK DKO are included in different images. Cell viability was determined by real-time imaging of cells simultaneous stained for total cells and dead cells. Data are shown as the mean ± SEM from a single experiment with ten technical replicates. The data are from one of two biological replicates. Significance was determined by two-way ANOVA. ***$p < 0.001$; ns, not significant.

(I) WT and RNase L KO A549 cells (as indicated) were transfected with 2-5A oligomers and incubated (1.5 h). Lysates were digested with micrococcal nuclease (MNase) and separated on a linear sucrose gradient to highlight collided ribosomes. Ultraviolet (UV) absorbance was measured with a fraction collector, and arrows highlight the peaks corresponding to di- and tri-somes (left and right arrows, respectively). The data are from one of two biological replicates. Control, untreated cells.

See also Figures S6 and S7.

KEY RESOURCES TABLE

REAGENT or RESOURCE	SOURCE	IDENTIFIER
Antibodies		
Phospho-p38 MAPK (Thr180/Tyr182) (D3F9) XP® Rabbit Monoclonal Antibody	Cell Signaling Technology	4511; RRID:AB_2139682
p38 MAPK Polyclonal Rabbit Antibody	Cell Signaling Technology	9212s; RRID:AB_330713
Phospho-SAPK/JNK (Thr183/Tyr185) (G9) Mouse Monoclonal Antibody	Cell Signaling Technology	9255; RRID:AB_2307321
SAPK/JNK Rabbit Polyclonal Antibody	Cell Signaling Technology	9252; RRID:AB_2250373
Phospho-p44/42 MAPK (Erk1/2) (Thr202/Tyr204) Rabbit Polyclonal Antibody	Cell Signaling Technology	9101; RRID:AB_331646
p44/42 MAPK (Erk1/2) (137F5) Rabbit Monoclonal Antibody	Cell Signaling Technology	4695; RRID:AB_390779
PARP Rabbit Polyclonal Antibody	Cell Signaling Technology	9542; RRID:AB_2160739
Cleaved PARP (Asp214) (D64E10) XP® Rabbit Monoclonal Antibody	Cell Signaling Technology	5625; RRID:AB_10699459
Mouse RNase L Rabbit Polyclonal Antibody	Banerjee et al.[28]	N/A
Human RNase L mouse Monoclonal Antibody	Dong and Silverman[14]	N/A
Mouse, Human ZAK Polyclonal Rabbit antibody	Proteintech	14945–1-AP; RRID:AB_10642698
Human ZAK Polyclonal Rabbit Antibody	Thermo Fisher Scientific (Bethyl Laboratories)	A301–993A; RRID:AB_1576612
Anti-a-Tubulin mouse Monoclonal Antibody	Sigma-Aldrich	T9026; RRID:AB_477593
FosB(5G4) Rabbit Monoclonal Antibody	Cell Signaling Technology	2251 RRID:AB_2106903
IL-1b (3A6) Mouse Monoclonal Antibody	Cell Signaling Technology	12242 RRID:AB_2715503
c-JUN(60A8) Rabbit Monoclonal Antibody	Cell Signaling Technology	9165 RRID:AB_130165
PKR Antibody (B-10)	Santa Cruz Biotechnology	Sc-6282 RRID:AB_628150
Phospho-MKK3(Ser189)/MKK6(Ser207) Antibody	Cell Signaling Technology	9231 RRID:AB_2140799
MKK3(D4C3) Rabbit Monoclonal Antibody	Cell Signaling Technology	8535 RRID:AB_11220233
Phospho-SEK1/MKK4(Ser 257/Thr261) Antibody	Cell Signaling Technology	9156 RRID:AB_2297420
SEK1/MKK4 Antibody	Cell Signaling Technology	9152 RRID:AB_330905
Chemicals, peptides, and recombinant proteins		
Poly(I):poly(C) (pIC)	Millipore Sigma	528906
JNK inhibitor (SP600125; CAS 129–56-6)	Santa Cruz Biotechnology	sc-200635
p38 inhibitor (SB203580; CAS 152121–47-6)	Millipore Sigma	559389
AP-1/NF-kB Dual Inhibitor (SP100030)	Millipore Sigma	5315350001
IKKa inhibitor (BAY 11–7082; CAS 19542–67-7)	Santa Cruz Biotechnology	sc-200615B
ZAK inhibitor 3h	Chang et al.[30]; Yang et al.[39]; Xiaoyun Lu, Jinan University, Guangzhou	N/A
ZAK inhibitor 6p	Chang et al.[30]; Yang et al.[39]; Xiaoyun Lu, Jinan University, Guangzhou	N/A

REAGENT or RESOURCE	SOURCE	IDENTIFIER
Anisomycin	Millipore Sigma	A9789
Lipofectamine 2000	ThermoFisher/Invitrogen	11668500
Lipofectamine 3000	ThermoFisher/Invitrogen	L3000001
Syto™ 60 red fluorescent nucleic acid stain	ThermoFisher/Invitrogen	S11342
Sytox™ green nucleic acid stain	ThermoFisher/Invitrogen	S7020
EZ-10 Spin Columns Total RNA Minipreps Super Kit	Bio Basic	BS583
High-capacity cDNA reverse transcriptase Kit	ThermoFisher/Applied Biosystems™	4368814
Bullseye EvaGreen qPCR 2x MasterMix-ROX	MidSci	BEQPCR-R
ACK Lysing Buffer	ThermoFisher/Gibco	A10492–01
recombinant murine M-CSF	ThermoFisher/Peprotech	315–02
Phos-Tag SDS-PAGE	Fujifilm Wako Chemicals U.S.A. Corp	AAL-107
Micrococcal nuclease (MNase)	New England Biolabs	#M0247
RiboLock RNase Inhibitor	Thermo Fisher Scientific	#EO0382
Protease inhibitor cocktail	Sigma-Aldrich	#P2714
Deposited data		
RNA sequencing data	This study	GEO: GSE253530
Experimental models: Cell lines		
THP-1	ATCC	TIB-202
THP-1 WT (control lentivirus-infected cells)	This study	N/A
THP-1 RNase L KO	This study	N/A
THP-1 ZAKa KO	This study	N/A
A549	ATCC	CCL-185
A549 WT (control lentivirus-infected cells)	This study	N/A
A549 RNase L KO	This study	N/A
A549 ZAKa KO	This study	N/A
A549 RNase L/ZAKa DKO	This study	N/A
A549 MAVS KO	Li et al.[43]; Roth-Cross et al.[59]; Susan Weiss, University of Pennsylvania	N/A
293T	ATCC	CRL-3216
Experimental models: Organisms/strains		
Male mice C57BL/6 WT	Jackson Laboratory	000664
Male mice C57BL/6 RNase L KO	Zhou et al.[50]; Leitner et al.[60].	N/A
Male mice C57BL/6 ZAK KO	Snieckute et al.[54]	N/A
Oligonucleotides		
See Table S1 for primer sequences See method details for 2',5'-oligoadenylates (2-5A)		
Recombinant DNA		

REAGENT or RESOURCE	SOURCE	IDENTIFIER
lentiCRISPR v2	Sanjana et al.[61]; Addgene, Feng Zhang	plasmid # 52961; RRID:Addgene_52961
psPAX2	Addgene, Didier Trono	plasmid # 12260; RRID:Addgene_12260
pCMV-VSV-G	Stewart et al.[62]; Addgene, Bob Weinberg	plasmid # 8454; RRID:Addgene_8454
Software and algorithms		
Cutadapt	Martin et al.[63]	Version 2.8
STAR	Dobin et al.[64]	Version 2.7.5a
DESeq2	Love et al.[65]	Version 1.30.1
DEXSeq	Anders et al.[66]; Reyes et al.[67]	Version 1.36.0
GSEA	Subramanian et al.[68]; Mootha et al.[68,69]	Version 4.1.0
R	The Comprehensive R Archive Network	Version 4.0.4